



This paper is a part of the hereunder thematic dossier published in OGST Journal, Vol. 70, No. 1, pp. 3-211 and available online [here](#)

Cet article fait partie du dossier thématique ci-dessous publié dans la revue OGST, Vol. 70, n°1, pp. 3-211 et téléchargeable [ici](#)

DOSSIER Edited by/Sous la direction de : **B. Leduc et P. Tona**

*IFP Energies nouvelles International Conference / Les Rencontres Scientifiques d'IFP Energies nouvelles E-COSM'12 — IFAC Workshop on Engine and Powertrain Control, Simulation and Modeling E-COSM'12 — Séminaire de l'IFAC sur le contrôle, la simulation et la modélisation des moteurs et groupes moto-propulseurs*

*Oil & Gas Science and Technology – Rev. IFP Energies nouvelles*, Vol. 70 (2015), No. 1, pp. 3-211

Copyright © 2015, IFP Energies nouvelles

- 3 > Editorial  
B. Leduc and P. Tona
- 15 > *A Challenging Future for the IC Engine: New Technologies and the Control Role*  
Un challenge pour le futur du moteur à combustion interne : nouvelles technologies et rôle du contrôle moteur  
F. Payri, J. M. Luján, C. Guardiola and B. Pla
- 31 > *The Art of Control Engineering: Science Meets Industrial Reality*  
L'art du génie automatique : science en rencontre avec la réalité industrielle  
U. Christen and R. Busch
- 41 > *Energy Management of Hybrid Electric Vehicles: 15 Years of Development at the Ohio State University*  
Gestion énergétique des véhicules hybrides électriques : 15 ans de développement à l'université d'État de l'Ohio  
G. Rizzoni and S. Onori
- 55 > *Automotive Catalyst State Diagnosis using Microwaves*  
Diagnostic de l'état de catalyseurs d'automobiles à l'aide de micro-ondes  
R. Moos and G. Fischerauer
- 67 > *Control-Oriented Models for Real-Time Simulation of Automotive Transmission Systems*  
Modélisation orientée-contrôle pour la simulation en temps réel des systèmes de transmission automobile  
N. Cavina, E. Corti, F. Marcigliano, D. Olivi and L. Poggio
- 91 > *Combustion Noise and Pollutants Prediction for Injection Pattern and Exhaust Gas Recirculation Tuning in an Automotive Common-Rail Diesel Engine*  
Prédiction du bruit de combustion et des polluants pour le réglage des paramètres d'injection et de l'EGR (*Exhaust Gas Recirculation*) dans un moteur Diesel *Common-Rail* pour l'automobile  
I. Arsie, R. Di Leo, C. Pianese and M. De Cesare
- 111 > *Investigation of Cycle-to-Cycle Variability of NO in Homogeneous Combustion*  
Enquête de la variabilité cycle-à-cycle du NO dans la combustion homogène  
A. Karvountzis-Kontakiotis and L. Ntziachristos
- 125 > *Energy Management Strategies for Diesel Hybrid Electric Vehicle*  
Lois de gestion de l'énergie pour le véhicule hybride Diesel  
O. Grondin, L. Thibault and C. Quérel
- 143 > *Integrated Energy and Emission Management for Diesel Engines with Waste Heat Recovery Using Dynamic Models*  
Une stratégie intégrée de gestion des émissions et de l'énergie pour un moteur Diesel avec un système WHR (*Waste Heat Recovery*)  
F. Willems, F. Kupper, G. Rascanu and E. Feru
- 159 > *Development of Look-Ahead Controller Concepts for a Wheel Loader Application*  
Développement de concepts d'une commande prédictive, destinée à une application pour chargeur sur pneus  
T. Nilsson, A. Fröberg and J. Åslund
- 179 > *Design Methodology of Camshaft Driven Charge Valves for Pneumatic Engine Starts*  
Méthodologie pour le design des valves de chargement opérées par arbre à cames  
M.M. Moser, C. Voser, C.H. Onder and L. Guzzella
- 195 > *Design and Evaluation of Energy Management using Map-Based ECMS for the PHEV Benchmark*  
Conception et évaluation de la gestion de l'énergie en utilisant l'ECMS (stratégie de minimisation de la consommation équivalente) basée sur des cartes, afin de tester les véhicules hybrides électriques rechargeables  
M. Sivertsson and L. Eriksson

# Control-Oriented Models for Real-Time Simulation of Automotive Transmission Systems

N. Cavina<sup>1\*</sup>, E. Corti<sup>1</sup>, F. Marcigliano<sup>2</sup>, D. Olivi<sup>1</sup> and L. Poggio<sup>2</sup>

<sup>1</sup> DIN, University of Bologna, Viale Risorgimento 2, 40136 Bologna - Italy

<sup>2</sup> Ferrari SpA, Via Abetone Inferiore 4, 41053 Maranello (MO) - Italy

e-mail: nicolo.cavina@unibo.it - enrico.corti2@unibo.it - francesco.marcigliano@ferrari.com - davide.olivi3@unibo.it  
luca.poggio@ferrari.com

\* Corresponding author

**Abstract** — A control-oriented model of a Dual Clutch Transmission (DCT) was developed for real-time Hardware In the Loop (HIL) applications, to support model-based development of the DCT controller and to systematically test its performance. The model is an innovative attempt to reproduce the fast dynamics of the actuation system while maintaining a simulation step size large enough for real-time applications. The model comprehends a detailed physical description of hydraulic circuit, clutches, synchronizers and gears, and simplified vehicle and internal combustion engine sub-models. As the oil circulating in the system has a large bulk modulus, the pressure dynamics are very fast, possibly causing instability in a real-time simulation; the same challenge involves the servo valves dynamics, due to the very small masses of the moving elements. Therefore, the hydraulic circuit model has been modified and simplified without losing physical validity, in order to adapt it to the real-time simulation requirements. The results of offline simulations have been compared to on-board measurements to verify the validity of the developed model, which was then implemented in a HIL system and connected to the Transmission Control Unit (TCU). Several tests have been performed on the HIL simulator, to verify the TCU performance: electrical failure tests on sensors and actuators, hydraulic and mechanical failure tests on hydraulic valves, clutches and synchronizers, and application tests comprehending all the main features of the control actions performed by the TCU. Being based on physical laws, in every condition the model simulates a plausible reaction of the system. A test automation procedure has finally been developed to permit the execution of a pattern of tests without the interaction of the user; perfectly repeatable tests can be performed for non-regression verification, allowing the testing of new software releases in fully automatic mode.

**Résumé** — **Modélisation orientée-contrôle pour la simulation en temps réel des systèmes de transmission automobile** — Un modèle orienté vers le contrôle d'une transmission à double embrayage (DCT, *Dual Clutch Transmission*) a été développé et implémenté en temps réel dans un système *Hardware In the Loop* (HIL), pour supporter le développement du contrôleur DCT et pour tester systématiquement ses performances. Le modèle représente une tentative innovatrice de reproduire les dynamiques rapides du système d'actionnement tout en conservant une dimension de pas de calcul assez grande pour l'application en temps réel. Le modèle comprend une description physique détaillée du circuit hydraulique, des embrayages, des synchroniseurs et des engrenages, et des sous-modèles simplifiés du véhicule et du moteur à combustion interne. Comme l'huile circulant dans le système est caractérisée par un module de compressibilité élevé, les dynamiques de pression sont très rapides, pouvant provoquer une

instabilité dans la simulation en temps réel, et le même risque intéresse la dynamique des servovalves, en raison des très petites masses des éléments mobiles. Par conséquent, le modèle de circuit hydraulique a été modifié et simplifié sans perdre la validité physique. Les résultats des simulations hors ligne ont été comparés à des mesures en ligne pour vérifier la validité du modèle, qui a ensuite été implémenté dans un système HIL et connecté à l'unité de control de la transmission (TCU, *Transmission Control Unit*). Plusieurs tests ont été effectués sur le simulateur HIL, pour vérifier la performance de la TCU : tests de panne électrique sur capteurs et actionneurs, tests de défaillance sur les valves hydrauliques, les embrayages et les synchros, et tests d'applications comprenant toutes les principales actions de contrôle effectuées par la TCU. Étant basé sur des lois physiques, dans toutes les conditions le modèle simule une réaction plausible du système. Une procédure d'automatisation de test a finalement été développée pour permettre l'exécution d'une suite de tests sans interaction de l'utilisateur; les tests parfaitement reproductibles peuvent être effectués pour la vérification de non régression, ce qui permet la validation de nouvelles versions du logiciel en mode entièrement automatique.

## NOMENCLATURE

ADC	Analog/Digital Converter
AMT	Automated Manual Transmissions
AT	Automatic Transmission
CVT	Continuously Variable Transmissions
DAC	Digital/Analog Converter
DCT	Dual Clutch Transmission
D/R	Digital/Resistance
ECU	Engine Control Unit
FIU	Failure Injection Unit
HIL	Hardware In the Loop
PWM	Pulse Width Modulation
RTP	Real-Time Processor unit
TCU	Transmission Control Unit

## INTRODUCTION

In recent years the need for increased fuel efficiency, driving performance and comfort has driven the development of engine and transmission technology in the automotive industry, and several types of transmissions are currently available in the market trying to meet these needs. The conventional Automatic Transmission (AT), with torque converter and planetary gears, was leading the market of non-manual transmissions, but in recent years it is losing its predominant position, because of the low efficiency of the converter and the overall structure complexity, in favour of other technologies. Continuously Variable Transmissions (CVT) permit avoiding the problem of gear shifting, but are limited in torque capacity and have the disadvantage of a low transmission efficiency due to the high pump losses caused by

the large oil flows and pressure values needed. Automated Manual Transmissions (AMT) with dry clutches are the most efficient systems, but they do not meet customer expectations due to torque interruption during gear shift (Zhang *et al.*, 2005). If compared to other transmissions, the DCT technology has the advantage of being suitable both for low revving and high torque Diesel engines, and for high revving engines for sport cars, maintaining a high transmission efficiency, as well as high gear shift performance and comfort (Matthes, 2005; Goetz *et al.*, 2005). A Dual Clutch Transmission can be considered as an evolution of the AMT. An AMT is similar to a manual transmission, but the clutch actuation and the gear selection are performed by electro-hydraulic valves controlled by a TCU (Transmission Control Unit). The peculiarity of a DCT system is the removal of torque interruption during gear shift typical of AMT, through the use of two clutches: each clutch is connected on one side to the engine, and on the other side to its own primary shaft, carrying odd and even gears, respectively.

The role of engine and transmission electronic control units is steeply increasing, and new instruments are needed to support their development. Hardware In the Loop (HIL) systems are nowadays largely used in the automotive industry, in which the crucial role of electronic control systems requires new techniques for software testing and validation. HIL systems are designed for testing control units in a simulation environment, allowing to perform functional and failure tests on the control unit, by connecting it to a device able to simulate the behavior of the controlled system (engine, transmission system, vehicle, etc.) in real-time.

The aim of this work is the development of a control-oriented model of a DCT system designed to

support model-based development of the DCT controller. The main original contribution of this work is a complete, real-time model of the hydraulic actuation circuit and of the DCT kinematics and dynamics, designed with a control-oriented approach. With respect to existing publications (Lucente *et al.*, 2007; Montanari *et al.*, 2004), the presented model (Cavina *et al.*, 2012) is in fact an innovative attempt to reproduce the fast dynamics of the actuation system while maintaining physical equations with a simulation step size large enough for real-time applications.

The model has been developed in Simulink environment; the reason for using such tool is twofold: Simulink allows the user to fully define the differential equations that represent the dynamic behavior of each component, allowing the introduction of mathematical simplifications when needed, without losing the physical validity of the simulation. Also, Simulink models are easily implemented in a fixed-step simulation model (which is necessary due to real-time constraints), and may be seamlessly integrated in the dSPACE HIL environment.

The developed model has been integrated in a Hardware In the Loop application for real-time simulation and the test of different software releases implemented inside the TCU is being carried out (Cavina *et al.*, 2013). Test automation permits executing tests at the simulator without the interaction of the user; the complete repeatability of every test is fundamental for non-regression tests on new software releases; the possibility to plan in advance the sequence of actions that have to take place during the test permits to execute tests that would not be possible with the manual interaction of the user.

The paper introduces the main aspects of the project, and provides further insight both into modeling and application areas. All the elements of the model are presented, including detailed descriptions of synchronizers, clutch and vehicle sub-models, and a new (and more accurate) clutch torque model, based on separators temperature estimation. Also, complex phenomena (such as for example clutch hysteresis) and the resulting modeling issues have been discussed and clarified. Finally, all relevant HIL tests are discussed in the second part of the paper, demonstrating the potential of model-based real-time simulation.

## 1 SYSTEM DESCRIPTION

In the system considered in this paper, shown in Figure 1, the two secondary shafts carry four synchronizers and

eight different gears (1<sup>st</sup>-7<sup>th</sup> and reverse). Thanks to the coordinated use of the two clutches, at the moment of gear shift the future gear is already preselected by the synchronizer on the shaft that is not transmitting torque; the only action performed during the gear shift is the opening of the currently closed clutch and the closing of the other one. Thanks to the control of clutch slips, the shifting characteristic is similar to the clutch-to-clutch shift commonly seen in conventional automatic transmissions (Kulkarni *et al.*, 2007); while in a conventional AT the gear shift smoothness is achieved through the action of the torque converter, which provides a dampening effect during shift transients, in a DCT transmission the shift comfort depends only on the control of clutch actuation (Liu *et al.*, 2009). The gearbox is actuated by a hydraulic circuit controlled by the TCU and divided in two different parts, one carrying the two clutches and the relative actuation and lubrication circuit, and the other actuating the four gear selectors.

### 1.1 Hydraulic Circuit Model

The hydraulic circuit scheme is shown in Figure 2. A rotative pump, directly connected to the engine *via* a fixed gear ratio, provides the necessary pressure level to the circuit, in which two different parts can be distinguished. The high pressure circuit provides oil to all servo valves that need a fast and well-calibrated actuation: clutch pressure control valves, which connect the high pressure circuit to the clutch pressure one, and gear selector valves, which feed the gear actuation circuit. The parking lock circuit and electronic differential one are also connected to the high pressure circuit.

The low pressure circuit, instead, controls the clutch lubrication; the lubrication oil, heated up by the thermal power generated in the clutches during their slip, is cooled down by a cooling system. The low pressure circuit is connected to the high pressure one through an orifice controlled by a servo valve: in this way the desired high pressure value can be controlled. If there is no need for oil in the circuit, the flow coming from the pump can be discharged to the sump thanks to the bypass circuit.

A generic pressure dynamics model was developed by considering the continuity equation of an incompressible fluid (Merritt, 1967), taking into account all input flows  $Q_{in}$  and output flows  $Q_{out}$  in the circuit, the total volume change from the initial value  $V_0$  caused by the motion of mechanical parts, and the total bulk modulus  $\beta_{tot}$  of the oil circulating in the circuit, as shown in:

$$Q_{in} - Q_{out} - \frac{dV_0}{dt} = \frac{V_0}{\beta_{tot}} \frac{dp}{dt} \quad (1)$$



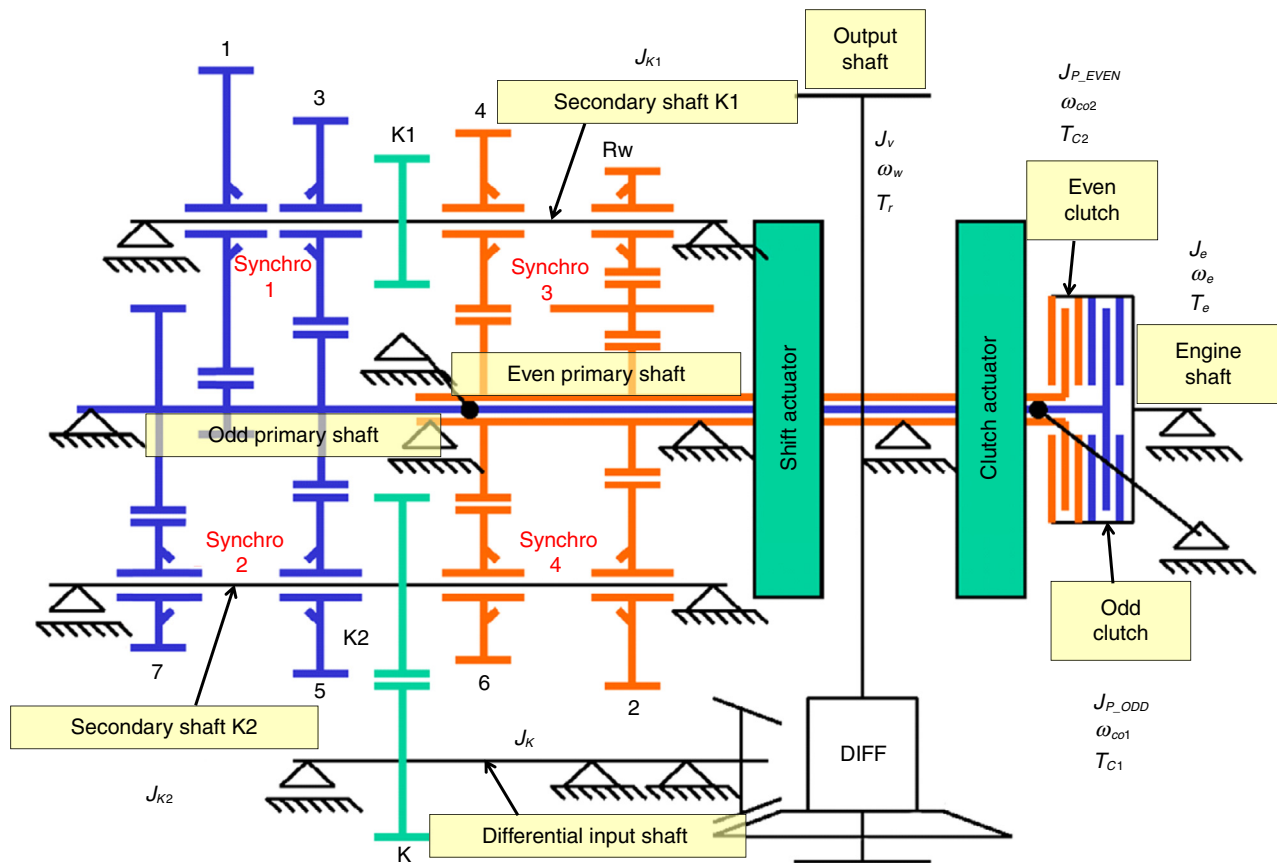


Figure 1  
Dual Clutch Transmission (DCT) layout.

Equation (1) can be applied for every part of the circuit: in the high pressure circuit, the term  $dV_0/dt$  can be considered negligible, because only the valve spools are moving and the volume change is very low. Instead, this term is particularly important in the clutch pressure circuit, because of the clutch motion while closing or opening, and in the synchronizers' actuation circuit, due to the rod motion from a position to another (depending on the selected gear).

## 1.2 System Pressure Model

The system pressure value (*i.e.* the pressure level in the high pressure circuit) is calculated according to Equation (1). The control of the system pressure is performed by regulating the actuation current on a servo valve; its output flow actuates a hydraulic valve, which opens the orifice that connects the high pressure

circuit to the low pressure one. This part of the hydraulic circuit comprehends several flows and small orifices; consequently, to develop a model suitable for real-time applications, the calculation of the flow from the high pressure circuit to the low pressure one is provided by an experimental map rather than by a dynamic model. Inputs to such map are the current applied to the servo valve and the pressure level in the high pressure circuit. Furthermore, the input flow  $Q_{in}$  provided by the pump is calculated *via* an experimental map depending on engine speed, and considering also leakage flows, which depend on the pressure level in the high pressure circuit. All other flows needed for the calculation of the system pressure value, *i.e.* flows from the high pressure circuit to the clutch pressure circuit and to the gear actuation circuit, are dynamically calculated considering the servo valves model, as explained in the next paragraphs (Eq. 4).

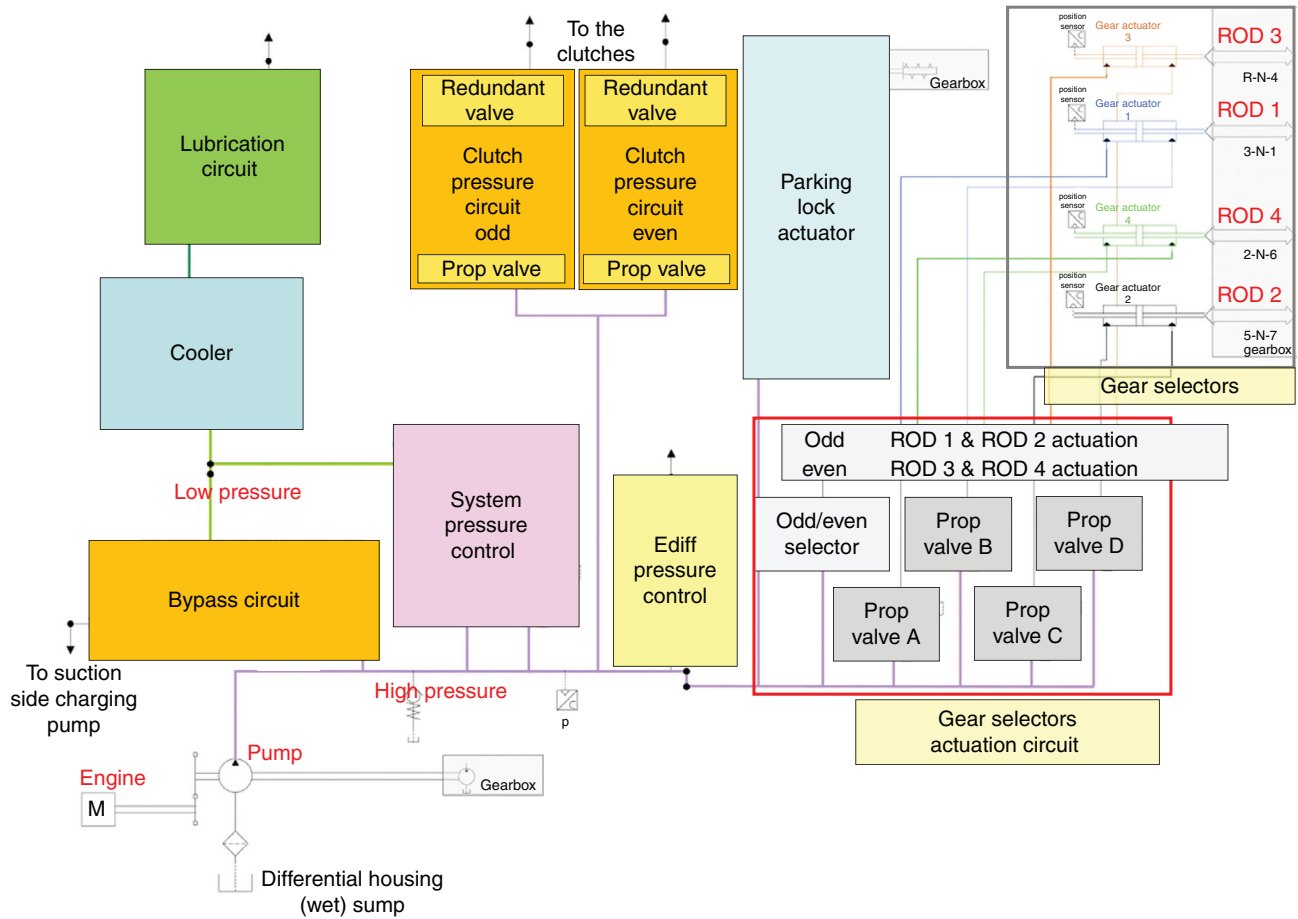


Figure 2  
Hydraulic circuit layout.

### 1.3 Pressure Control Valve Model

The pressure level acting on clutches and gear actuators is controlled by proportional pressure control valves (Fig. 3), which are designed to act as closed loop systems (Lucente et al., 2007): the proportionality between actuation current on the solenoid and pressure in the actuation chamber  $p_A$  is given by the feedback chamber, which generates a feedback force  $F_{fb}$  against the valve opening, whose proportionality factor is the feedback chamber area  $A_{fb}$  of the spool, as shown in:

$$F_{fb} = p_A A_{fb} \quad (2)$$

The spool dynamics may be described by the mass-spring-damper analogy, as in:

$$m_{sp} \ddot{x}_{sp} + b_{sp} \dot{x}_{sp} + k_{sp} x_{sp} = F_{sol} - F_{fb} - F_{fl} - F_{pr\_sp} \quad (3)$$

The electromagnetic force on the spool  $F_{sol}$  has been experimentally characterized, depending on the input current and on the spool position  $x_{sp}$ . The flow forces  $F_{fl}$  are calculated using experimental data, depending on flow, valve position and pressure difference between input and output ports. The spring preload  $F_{pr\_sp}$  modifies the pressure range in which there is proportionality between current and pressure.

When there is no current acting on the solenoid, the actuator port A is connected to the return port T and the oil from the actuation circuit flows to the oil sump (Fig. 3, 4a). By supplying current, the solenoid force rises and the spool is moved forward; the spool reaches a position in which the port A is connected neither to the port T nor to the port P; this position is called “Dead Zone Start”. Moving further, the spool connects the actuator port A to the inlet port P (Fig. 4b); the position of first connection between A and P is called “Dead Zone End”.

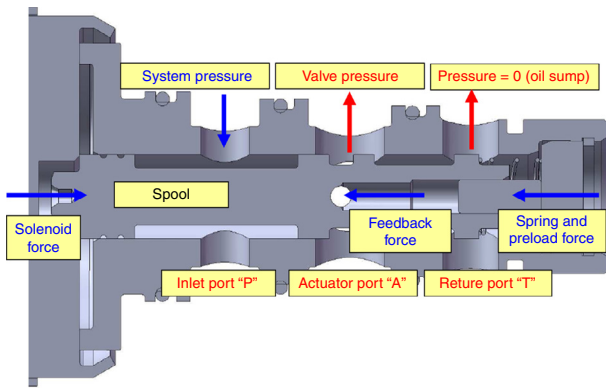


Figure 3  
Proportional 3-way pressure regulation valve.

The oil flow raises the pressure in the actuation chamber, and the feedback force rises as well, forcing the spool to move back to the “Dead Zone”, reaching the equilibrium position of the system (Fig. 4c).

The flow through the valve is given by (4), according to Bernoulli formulation for incompressible fluids (Lucente *et al.*, 2007; Montanari *et al.*, 2004):

$$Q(x_{sp}, \Delta p) = \begin{cases} -\text{sign}(p_A - p_T) n_A C_d A_A(x_{sp}) \sqrt{\frac{2|p_A - p_T|}{\rho_{oil}}} & \text{if } x_{sp} < x_{DeadZoneStart} \\ 0 & \text{if } x_{DeadZoneStart} \leq x_{sp} \leq x_{DeadZoneEnd} \\ \text{sign}(p_P - p_A) n_A C_d A_A(x_{sp}) \sqrt{\frac{2|p_P - p_A|}{\rho_{oil}}} & \text{if } x_{sp} > x_{DeadZoneEnd} \end{cases} \quad (4)$$

The effective area connecting the actuation port depends on the geometrical area  $A_A(x_{sp})$ , the number of orifices  $n_A$  and the discharge coefficient  $C_d$ . To avoid stability problems during the simulation, when the pressure difference is very low the Bernoulli Equation (4) is replaced by the parabolic Equation (5) that provides smaller flow values when  $|\Delta p| \leq \Delta p^*$  (a similar problem is solved with the same approach in Guzzella and Onder, 2004), as shown in Figure 5:

$$\text{if } |\Delta p| \leq \Delta p^*: \\ Q(x_{sp}, \Delta p) = \pm \text{sign}(\Delta p) n_A C_d A_A(x_{sp}) \sqrt{\frac{2\Delta p^*}{\rho_{oil}}} \frac{|\Delta p|^2}{\Delta p^2} \quad (5)$$

#### 1.4 Clutch Model

The clutches of the considered DCT are wet clutches; the lubrication oil removes the heat generated

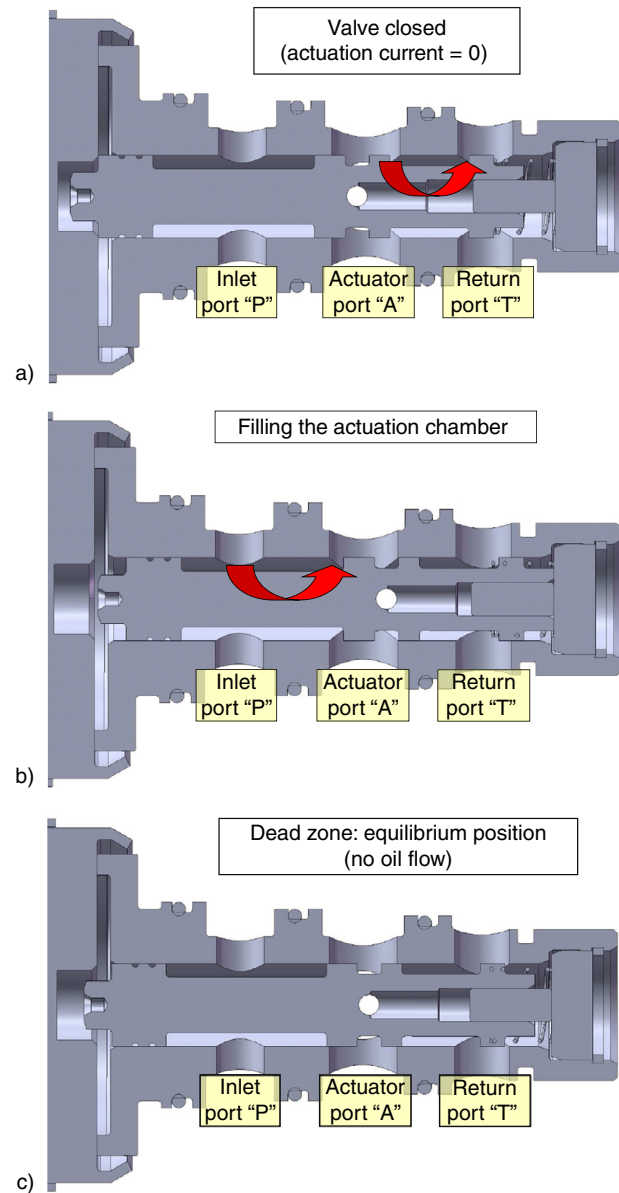


Figure 4  
Proportional 3-way valve motion.

while slipping, and torque is transmitted by the contact between the clutch discs, covered with high-friction materials, and the separator plates. The clutch motion is opposed by Bellville springs between every friction disc, giving also a preload force. For safety reasons, when no actuation is required, the clutch is open and engine shaft and transmission shaft are separated. The clutch closure is performed by pumping current in the

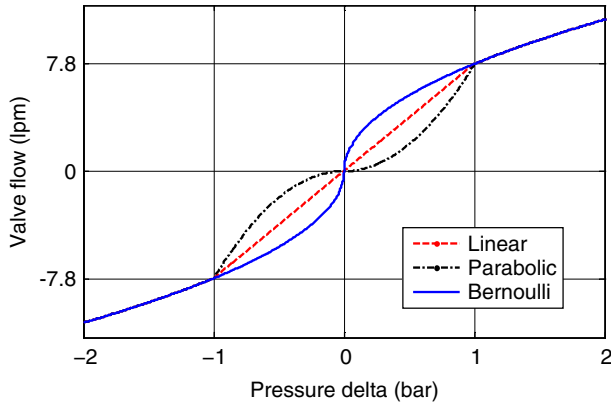


Figure 5  
Parabolic interpolation for Bernoulli equation.

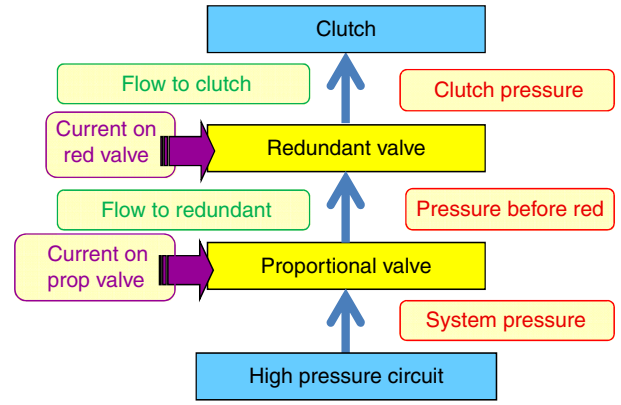


Figure 6  
Clutch actuation scheme.

corresponding proportional valve, in order to raise the pressure level acting on the clutch actuator.

The clutches are not directly connected to their proportional actuation valve; for safety reasons, between the clutches and the proportional valves that control the clutch pressure, two on/off valves (called “redundant valves”, Fig. 6), one for each clutch, permit the fast discharge of the oil from the clutch to the sump (and the consequent opening of the clutch) bypassing the other components of the circuit in case of fault, or when there is the need of opening the clutches as fast as possible during the gear shift. When no current is applied on the valves, they discharge the oil from the clutch actuation chamber to the sump; on the contrary, when current is supplied they allow the oil flow between the proportional valves and the clutches.

The redundant valve is constructively similar to the proportional one, but it presents an on/off behavior because of the absence of the feedback port; consequently, the position of the spool depends only on the current supplied to it; if the current level is high enough, it remains fully open, whatever pressure level is present in the actuation chamber. The dynamic model of the redundant valve spool motion is similar to the one of the proportional valve, but without the term which considers the feedback force:

$$m_{red}\ddot{x}_{red} + b_{red}\dot{x}_{red} + k_{red}x_{red} = F_{sol} - F_{fl} - F_{pr-red} \quad (6)$$

The model of clutch actuation circuit between the proportional valve and the clutch is divided in two different parts, in order to consider the pressure dynamics through the redundant valve that, even when its spool is not moving but steady in the position of full opening,

is not negligible (for example during the clutch filling transient). Calculation of the pressure  $p_{b\_red}$  in the chamber between the proportional valve and the redundant valve may be performed by applying the mass conservation principle of Equation (1), as shown in:

$$Q_{prop} - Q_{red} = \frac{V_{0b\_red}}{\beta} \frac{dp_{b\_red}}{dt} \quad (7)$$

Calculation of pressure  $p_c$  acting on the clutch may be performed in a similar way:

$$Q_{red} - Q_c - \frac{dV_{0c}}{dt} = \frac{V_{0c}}{\beta} \frac{dp_c}{dt} \quad (8)$$

The flow  $Q_c$  exiting the clutch is a leakage flow of oil going from the clutch actuation chamber back to the sump. This leakage flow is not negligible and it was designed to lubricate the clutch actuation moving elements. Its value is calculated according to an experimental map that takes into account the pressure in the actuation circuit and the oil temperature.

The volume change in the clutch, calculated in Equation (9), is not negligible while the clutch is being closed or opened; in this case, it can be evaluated by considering the longitudinal speed of the clutch  $\dot{x}_c$  calculated in Equation (10):

$$\frac{dV_{0c}}{dt} = \frac{d(A_c x_c)}{dt} = A_c \dot{x}_c \quad (9)$$

The clutch closure procedure can be divided into different phases. At first, the clutch is completely open; when a clutch closure is required, current is pumped to the relative proportional valve, maintaining the relative



redundant valve open; as soon as the oil reaches the clutch actuation chamber, the oil pressure inside the chamber rises, and consequently the force acting on the actuation piston, which is connected to the clutch discs. The clutch piston and discs longitudinal dynamics follows the mass-spring-damper Equation (10):

$$m_c \ddot{x}_c + b_c \dot{x}_c + k_c x_c = p_c A_c - F_{pr-c} \quad (10)$$

The clutch motion is contrasted by the resistant force  $k_c x_c$  coming from the Bellville springs. Experimental tests showed that it is not a fully linear relation; consequently an experimental map was obtained.

As soon as the oil in the actuation chamber reaches a level higher than the preload force  $F_{pr-c}$ , the clutch is forced to move forward. The resistant force consequently rises and the clutch stops until more oil (and pressure) is provided. Therefore, in this phase the pressure in the chamber is not proportional to the current on the proportional valve, but to the piston longitudinal position (“filling phase”). The lowest pressure level for which the clutch is completely closed (“kiss point pressure”) depends on preload pressure and spring stiffness. When the kiss point position is reached, the friction discs connected to the clutch output shaft and the separator plates connected to the clutch input shaft come in contact. Usually these two shafts have different speeds, and some friction torque is transmitted between them thanks to the friction material with which the discs are covered. From this moment, the pressure in the actuation chamber is directly proportional to the current on the valve. By exchanging torque, the two shafts synchronize their speeds, becoming a rigid system with only one degree of freedom; its final speed depends on the inertia of the two parts and on the applied torque.

### 1.5 Clutch Hysteresis

Analyzing Figure 7, which shows experimental data measured while actuating a current ramp on the valve, first rising and then falling, it can be noticed that the values of preload and kiss point pressure of the clutch are significantly different between the closing and the opening phase. This is due to the Coulomb friction between the clutch actuation seal and its seat: during the rising ramp, some force is needed to overtake the static force and move the clutch; consequently the pressure at the preload point is higher than during the falling ramp. When the clutch is completely closed some force is needed to move the clutch back through the action of the Belleville springs, and consequently a lower oil pressure level must be reached to start the clutch opening.

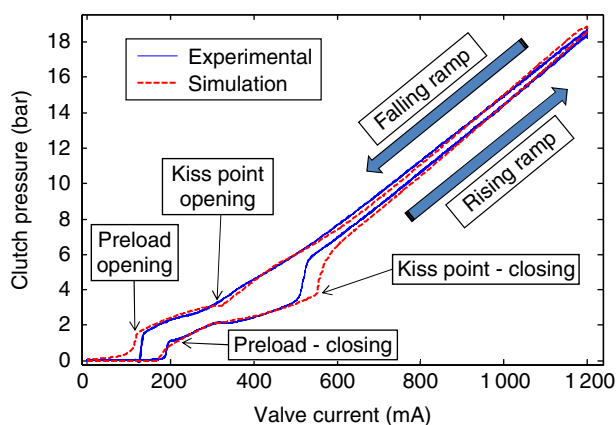


Figure 7

Rising and falling current ramp on clutch valve.

This consideration clarifies why the kiss point pressure is lower during the falling ramp.

Clutch hysteresis has been simulated in the model using two different levels of preload pressure for the two phases: the kiss point pressure level is a consequence of such choice, since once the preload level is defined, the kiss point pressure only depends on clutch spring stiffness. It is a rough simplification of a complex hysteretic behavior (Bertotti and Mayergoyz, 2006; Eyabi and Washington, 2006), but it is probably the most suitable, because of the real-time constraint and the lack of more experimental details about this phenomenon.

It can be also noticed that the relationship between actuation current and clutch pressure is not unique; it happens not only during the closing and opening phases, in which the process is ruled by the spring stiffness, but also at higher current values, for which the clutch is completely closed. This behavior is due to the fact that during the ramps the pressure variation is achieved by modifying the volume of oil inside the circuit. During a rising ramp, some oil flow has to enter the circuit, and the valve spool must be in a position that allows the connection between P and A ports (Fig. 4b). During a falling ramp, oil must be discharged to the sump, and the spool must be in a position that allows oil flow from port A to port T (Fig. 4a). Consequently, at the same pressure level, when the valve is filling the circuit the position of the spool is after the “Dead Zone”, while when the valve is discharging the circuit the spool is before the “Dead Zone”. In conclusion, during a rising phase more current is needed on the valve than during a falling phase, at the same pressure level, and it should be observed that in a static characterization of the valve this effect would

not be present. The developed model, being based on physical laws, is capable to correctly reproduce this phenomenon, as shown in Figure 7.

### 1.6 Clutch Torque

The evaluation of the torque transmitted by a wet friction clutch is a very delicate topic to deal with. Even the use of simplified equations based on the assumption of constant fluid thickness and constant temperature over the clutch area (Deur et al., 2005; Davis et al., 2000; Greenwood and Williamson, 1966) would be too complicated for a real-time control-oriented application.

Therefore, the clutch torque model used in this work is based on experimental maps (Fig. 8) depending on the clutch slip (i.e. the difference between the engine speed  $\omega_e$  and the clutch output speed  $\omega_{co}$ ) and on the “net” pressure acting on the clutch (the overall pressure level  $p_c$  decreased by the kiss point pressure  $p_{c\_kp}$ ). Different maps were obtained for different oil temperatures, and during the simulation such maps are interpolated by considering the actual oil temperature value. This torque value  $T_{cBasic}$ , called “Basic Torque”, is further modified by taking into account the current operating conditions, since the temperature of the clutch separators strongly influences the friction coefficient of the friction material.

The temperature inside the clutch is calculated through a linear mean value model, based on energy conservation principle (Lai, 2007; Velardocchia et al., 2000). The separators temperature  $T_{sep}$  is calculated by considering the net heat flow inside the clutches and the heat capacity  $m_{sep} c_{p\_sep}$  of the separators:

$$\begin{aligned} P_c - P_{oil} &= m_{sep} c_{p\_sep} \frac{dT_{sep}}{dt} \\ T_{sep} &= \int \frac{P_c - P_{oil}}{m_{sep} c_{p\_sep}} dt \end{aligned} \quad (11)$$

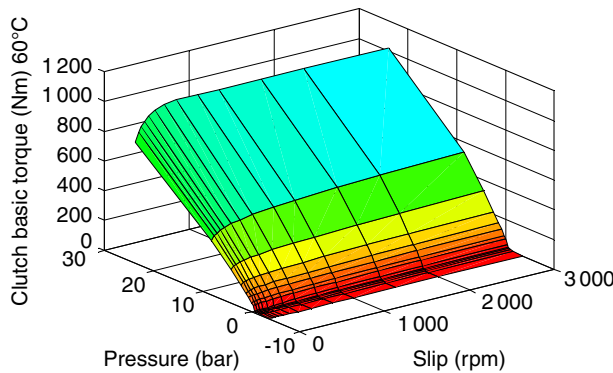


Figure 8  
Clutch basic torque (oil temperature 60°C).

The heat power generated inside the clutches  $P_c$  is a consequence of the clutch discs slip and of the transmitted torque  $T_c$ ; the heat power removed from the clutches by the lubrication oil  $P_{oil}$  depends on the amount of lubrication flow  $Q_{lb}$  and on the specific heat of the oil  $c_{p\_oil}$ :

$$P_c = (\omega_e - \omega_{co})T_c \quad (12)$$

$$P_{oil} = Q_{lb}c_{p\_oil}(T_{oil} - T_{cooler}) \quad (13)$$

where  $T_{cooler}$  is the temperature of the oil out of the cooling system, that is assumed to be constant. An experimentally-derived function  $f(Q_{lb})$  permits determining the temperature  $T_{oil}$  of the oil inside the clutches, if the temperature of the separators is known:

$$T_{oil} = T_{sep} - (T_{sep} - T_{cooler})f(Q_{lb}) \quad (14)$$

The variation of the clutch friction coefficient  $\Delta\mu_c(T_{sep}, \omega_e - \omega_{co})$ , according to the temperature of the clutch separators and to the amount of slipping, was experimentally determined and used to calculate its effect  $\Delta T_{cTsep}$  on transmitted torque:

$$\Delta T_{cTsep} = p_c A_c r_{mc} \Delta\mu_c \quad (15)$$

where  $r_{mc}$  is the clutch mean radius.

The total friction torque  $T_{cFrict}$ , generated by the friction between the clutch discs, can therefore be expressed as:

$$T_{cFrict} = T_{cBasic} + \Delta T_{cTsep} \quad (16)$$

When the pressure on the clutch is lower than the kiss point pressure, the clutch is not completely closed, and the drag torque  $T_{cDrag}$ , due to the viscosity of the oil inside the clutches, must be taken into account (it has been experimentally determined, depending on engine speed, clutch output speed, lube flow and oil temperature). Finally, the two clutches are not completely independent, being influenced by their mutual movement: an experimentally derived crosstalk torque  $\Delta T_{cCross}$  is added to the total torque, depending on the clutch pressure. All these terms contribute to the calculation of the total transmitted torque  $T_c$ .

### 1.7 Synchronizers Model

The synchronizer mechanism consists of a gearshift sleeve with internal dog gearing, connected to the synchronizer body and to the transmission shaft, cone synchronizer rings with locking toothing, and a synchronizer hub with selector teeth and friction cone, connected

to the gear which is idle on the transmission shaft thanks to needle roller bearings (Naunheimer *et al.*, 2011; Neto *et al.*, 2006).

The four rods used for the motion of the four synchronizers are hydraulically actuated by the high pressure circuit, as shown in Figure 2. Their position is controlled by four proportional pressure control valves, whose features have been described before, and four hydraulic double acting pistons, each controlled by two of those valves, one controlling the pressure level of the left chamber, and the other one of the right chamber. Actuating alternatively one valve or the other, the rod can be moved towards the desired position; every synchronizer controls the engagement of two gears, and the central position of the rod corresponds to the freewheel position.

If the synchronizer is not engaging any gear and no pressure is applied on its actuation piston, the gearshift sleeve is held in the middle position by a detent. Between the two chambers of the double acting piston with area  $A_{rod}$  a pressure difference  $p_{rod}$  is determined by providing different pressure levels  $p_l$  and  $p_r$  on the left and right chamber, respectively:

$$p_{rod} = p_l - p_r \quad (17)$$

The selection between odd and even gears is executed by actuating an on/off valve, which moves a hydraulic selector, that remains in “odd” position if the valve is not actuated, while it moves to the “even” position if the valve is actuated. The developed model of this selector is a static model which calculates the position of the distributor according to the current on the valve and the system pressure level  $p_{sys}$ :

$$x_{sel} = \begin{cases} x_{0\_sel} & \text{if current} < \text{threshold} \\ x_{0\_sel} + \frac{p_{sys} A_{sel} - F_{pr\_sel}}{k_{sel}} & \text{if current} \geq \text{threshold} \end{cases} \quad (18)$$

where  $A_{sel}$  is the actual area for pressure,  $F_{pr\_sel}$  is the spring preload force and  $k_{sel}$  is the valve spring stiffness.

The pressure dynamics inside the chambers of the actuation piston can be calculated according to Equation (19), considering as input and output flows the ones coming from the valve model, while the leakage flow on the rod actuation chambers can be considered negligible:

$$Q_{in\_prop} - Q_{out\_prop} - \frac{dV_{0rod}}{dt} = \frac{V_{0rod}}{\beta} \frac{dp_{rod}}{dt} \quad (19)$$

The motion of the hydraulic piston and of the sleeve, shown in Figure 9, is described as a spring-mass-damper

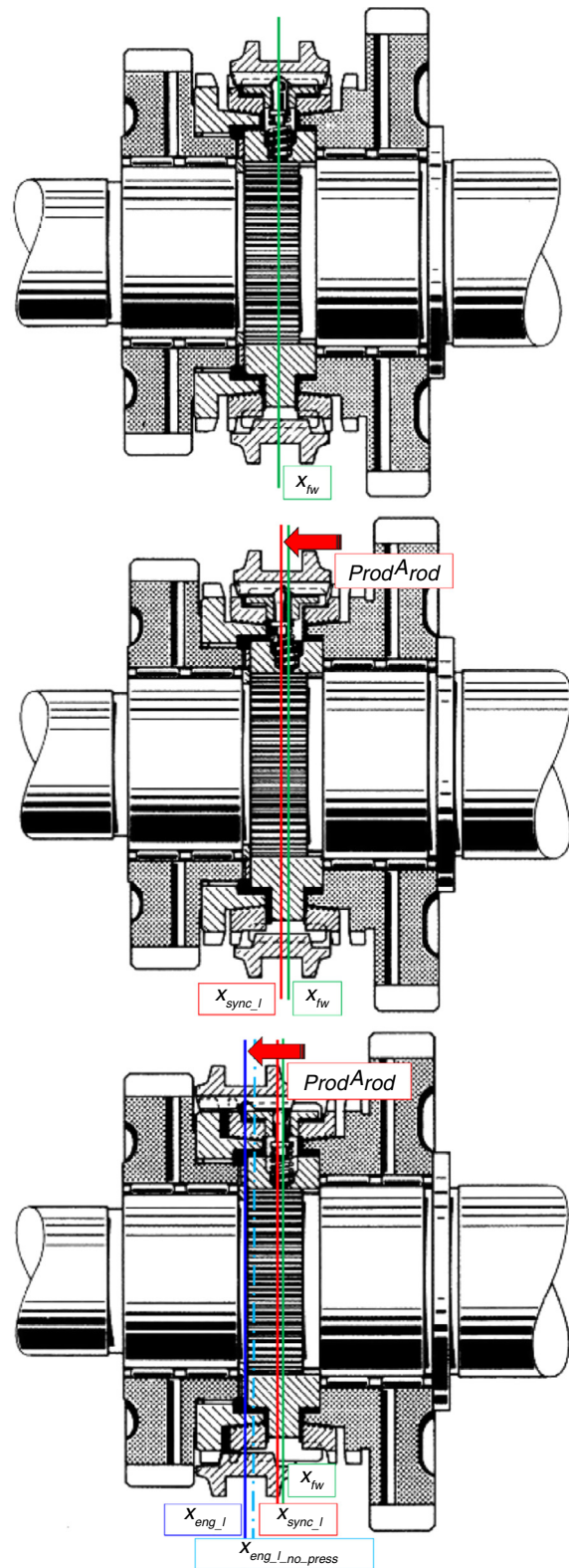


Figure 9

Synchronizing process: a) sleeve in freewheel position, no gear engaged; b) ring and hub synchronizing their speeds; c) sleeve on hub: left gear engaged.

dynamic equation. For simplicity, the coordinates taken into account are different depending on the position of the sleeve of the synchronizer; the position  $x_{rod}$  can be considered the “absolute” position, *i.e.* the position value as registered by the on-board sensor and that has to be reproduced by the model, always increasing from the left engaged position  $x_{l\_eng}$  to the right engaged position  $x_{r\_eng}$ ;  $x_{eng\_l\_no\_press}$  and  $x_{eng\_r\_no\_press}$  are the engaged positions when no pressure is applied on the actuation piston anymore. The position  $x_{fw}$  is the free-wheel position of the sleeve, when no gear is selected. The different chosen intervals correspond to different phases:

$x_1 = x_{rod} - x_{eng\_l\_no\_press}$  when  $x_{eng\_l} < x < x_{sync\_l}$ ;  
in this interval the left gear is selected:

$$m_{rod}\ddot{x}_1 + b_{rod}\dot{x}_1 + k_{eng}x_1 = p_{rod}A_{rod} \quad (20)$$

$x_2 = x_{rod} - x_{fw}$  when  $x_{sync\_l} < x < x_{sync\_r}$ ;  
in this interval no gear is selected:

$$m_{rod}\ddot{x}_2 + b_{rod}\dot{x}_2 + k_{fw}x_2 = p_{rod}A_{rod} \quad (21)$$

$x_3 = x_{rod} - x_{eng\_r\_no\_press}$  when  $x_{sync\_r} < x < x_{eng\_r}$ ;  
in this interval the right gear is selected:

$$m_{rod}\ddot{x}_3 + b_{rod}\dot{x}_3 + k_{eng}x_3 = p_{rod}A_{rod} \quad (22)$$

where  $k_{eng}$  is the spring stiffness imposed when the gear is in engaged position, and  $k_{fw}$  the one when it is in free-wheel position.

During the synchronization phase, the longitudinal motion of the rod is temporarily stopped in the position  $x_{sync\_l}$  or  $x_{sync\_r}$ , waiting for the speed synchronization between the synchronizer rings and the hub; the synchronizer sleeve and ring rotate at the same speed of the secondary shaft, and consequently their speed is dependent on the vehicle speed; the gear, instead, rotates according to the speed of the primary shaft; in this position torque is transmitted between the two elements. The longitudinal motion of the synchronizer can restart when the synchronization phase is over.

It is supposed that during the synchronization process the correspondent clutch is open; thus, the only resistant torque is the viscous friction of the primary shaft bearings. The speed of the synchronizing gear  $\omega_{gear}$  on the considered secondary shaft is given by Equation (23), depending on the relative primary inertia  $J_p$  referred to the secondary shaft, due to the gear ratio  $\tau_{gear}$  between the two shafts:

$$T_{syn} - b_p\omega_{gear} = J_p\tau_{gear}^2\dot{\omega}_{gear} \quad (23)$$

The torque  $T_{syn}$  exchanged between ring and hub can be calculated considering the torque transmitted by a cone friction clutch (Razzacki, 2004), according to the surface friction coefficient  $\mu_{syn}$ , the cone mean radius  $R_{m\_ring}$  and the cone angle  $\theta$ :

$$T_{syn} = \frac{p_{rod}A_{rod}\mu_{syn}R_{m\_ring}}{\sin(\theta)} \quad (24)$$

The viscous friction coefficient of primary shafts  $b_p$  was experimentally determined by analyzing the coast-down trend of the shaft, when the respective clutch is open, and the synchronizer is moved towards its free-wheel position, leaving the primary shaft and the gears free to slow down.

## 1.8 Vehicle Model

The vehicle model that has been designed and implemented for this project neglects elasticity effects of both shafts and tires, since the HIL simulator has been realized to support functionality analysis and software debugging of the DCT controller, rather than gearshift quality analysis (which is typically part of a drivability optimization activity carried out directly on the vehicle). For this reason, first order transmission system dynamics were not considered as an important feature to be included in the vehicle model, in an effort to keep it as simple (and fast) as possible; therefore, the implemented dynamic equations consider shafts with infinite stiffness.

The model consists of different sets of equations, depending on whether the clutch is completely closed or slipping, and further, whether a gear is currently selected, or not. The speeds of vehicle, gears and gearbox shafts are calculated by considering inertial effects and the torques acting on them (Kulkarni et al., 2007; Liu et al., 2009). When the clutch is completely closed and a gear is selected, engine, gearbox and vehicle are connected and only one differential equation provides the description of the entire system dynamics (under the hypothesis of infinite stiffness); the engine speed  $\omega_e$  is calculated considering the net torque on engine shaft, *i.e.* the difference between the engine torque  $T_e$  and the resistant torque  $T_r$ , properly divided by the total gear ratio  $\tau_{tot}$  of the currently selected gear:

$$T_e - \frac{T_r}{\tau_{tot}} = \left( J_e + J_{eq-p} + \frac{J_{eq-g}}{\tau_{tot}^2} \right) \dot{\omega}_e \quad (25)$$

For simplicity, the inertia  $J_e$  of all the elements before the clutch and the equivalent inertia of primary shafts



$J_{eq\_p}$  are referred to the engine shaft, while the equivalent inertia  $J_{eq\_g}$  of shafts  $K1$ ,  $K2$ ,  $K$  (Fig. 1) and of the whole vehicle are referred to the wheel shaft:

$$J_{eq\_p} = J_{eq\_p\_ODD} + J_{eq\_p\_EVEN} \quad (26)$$

$$J_{eq\_g} = J_{eq\_K1} + J_{eq\_K2} + J_{eq\_K} + J_{eq\_v} \quad (27)$$

The equivalent primary inertia is calculated from the inertia of primary shafts referred to their own axes; the equivalent value referred to the engine axes depends on the current gear, *i.e.* the gear whose clutch is closed and therefore transmitting torque to the wheels. The equivalent inertia is the axes inertia if the clutch of the considered gear is closed, otherwise a multiple gear ratio must be considered. If the current gear is odd:

$$J_{eq\_p\_ODD} = J_{p\_ODD}$$

$$J_{eq\_p\_EVEN} = \left( \frac{\tau_{k\_EVEN} \tau_{pres}}{\tau_{k\_ODD} \tau_{sel}} \right)^2 J_{p\_EVEN} \quad (28)$$

where  $\tau_{k\_ODD}$  is the gear ratio between the secondary shaft ( $K1$  or  $K2$ , depending on which odd gear is selected) and  $K$  shaft, the same for  $\tau_{k\_EVEN}$ , while  $\tau_{sel}$  is the total gear ratio of the currently selected gear and  $\tau_{pres}$  the one of the preselected gear on the other primary shaft. If the current gear is instead an even gear:

$$J_{eq\_p\_ODD} = \left( \frac{\tau_{k\_ODD} \tau_{pres}}{\tau_{k\_EVEN} \tau_{sel}} \right)^2 J_{p\_ODD}$$

$$J_{eq\_p\_EVEN} = J_{p\_EVEN} \quad (29)$$

The equivalent inertia of all the other shafts inside the gearbox (the secondary shafts and the differential input shaft) and the vehicle inertia are referred to the wheels, so the transmission ratio between the secondary shaft and the differential input shaft  $\tau_{K1}$  and  $\tau_{K2}$  and the differential ratio  $\tau_{diff}$  must be taken into account:

$$J_{eq\_K1} = J_{K1} (\tau_{K1} \tau_{diff})^2 \quad (30)$$

$$J_{eq\_K2} = J_{K2} (\tau_{K2} \tau_{diff})^2 \quad (31)$$

$$J_{eq\_K} = J_K \tau_{diff}^2 \quad (32)$$

$$J_{eq\_v} = M_v R_w^2 \quad (33)$$

where  $M_v$  is the vehicle total mass and  $R_w$  the wheel radius. The total transmission ratio is defined as the ratio between engine speed  $\omega_e$  and wheel speed  $\omega_w$ :

$$\tau_{tot} = \frac{\omega_e}{\omega_w} \quad (34)$$

The vehicle speed  $v$  is calculated considering the total gear ratio  $\tau_{tot}$  and the wheel radius  $R_w$  (assuming no wheel slip):

$$v = \frac{\omega_e}{\tau_{tot}} R_w \quad (35)$$

The resistant torque acting on the vehicle can be calculated following a simple standard approach (Guzzella and Sciarretta, 2008); it is due to the aerodynamic force (depending on air density  $\rho_a$ , frontal area of the vehicle  $A_v$  and vehicle drag coefficient  $C_x$ ), the rolling friction resistance (depending on rolling friction coefficient  $f_r$  and vehicle total mass  $M_v$ ) and the braking torque  $T_{br}$ :

$$T_r = \left( \frac{1}{2} \rho_a A_v C_x v^2 + f_r M_v g \right) R_w + T_{br} \quad (36)$$

Aerodynamic and rolling resistant torques can also be calculated considering the coast-down behavior of the vehicle, as shown in Equation (37), with the use of three curve fitting parameters  $f_0$ ,  $f_1$ ,  $f_2$ :

$$T_{aer} + T_{roll} = (f_0 + f_1 v + f_2 v^2) R_w \quad (37)$$

The braking torque is proportional to the pressure acting on the brake circuit, that is the pressure of the brake fluid  $p_{br}$  (proportional to the pressure on the brake pedal), the actual areas for pressure  $A_f$ ,  $A_r$  of front and rear discs respectively, the friction coefficients of the linings  $\mu_f$ ,  $\mu_r$ , and the mean radius of brake discs  $R_f$ ,  $R_r$ :

$$T_{br} = 2p_{br} A_f \mu_f R_f + 2p_{br} A_r \mu_r R_r \quad (38)$$

When the clutch is slipping, the system has one more degree of freedom; it must be divided into two different parts, one from the engine to the clutch (39), and the other (40) from the clutch to the wheels:

$$T_e - (T_{c1} + T_{c2}) = J_e \dot{\omega}_e \quad (39)$$

$$T_{c1} \tau_1 + T_{c2} \tau_2 - T_r = (J_{eq\_p} \tau_{tot}^2 + J_{eq\_g}) \dot{\omega}_w \quad (40)$$

where  $T_{c1}$  and  $T_{c2}$  are the torques respectively transmitted by clutch 1 and clutch 2. Equation (40) is referred to the wheel axes, thus the clutch torques must be multiplied by  $\tau_1$  and  $\tau_2$ , which are the total gear ratios of the currently selected gears on odd and even shafts, respectively:

$$\tau_1 = \frac{\omega_{co1}}{\omega_w}; \tau_2 = \frac{\omega_{co2}}{\omega_w} \quad (41)$$



where  $\omega_{co1}$  and  $\omega_{co2}$  represent the clutch output speeds.

A particular case that must be taken into account is when no gear is selected: the primary and secondary shafts of the gearbox are not connected anymore, adding one more degree of freedom to the system. The vehicle, not influenced by the clutch or engine torque anymore, slows down because of the resistant torque experienced during coast down:

$$-T_r = J_{eq-g}\dot{\omega}_w \quad (42)$$

The primary shafts are accelerated by the clutch torque; the dynamics are very fast because the only resistant torque is the viscous friction due to the bearings, and the primary shaft inertia is very low:

$$\begin{aligned} T_{c1} - b_p\omega_{co1} &= J_{p\_ODD}\dot{\omega}_{co1} \\ T_{c2} - b_p\omega_{co2} &= J_{p\_EVEN}\dot{\omega}_{co2} \end{aligned} \quad (43)$$

where the clutch torque  $T_{ci}$  is equal to the engine torque if the clutch is closed (slip = 0), or it is calculated by the clutch torque model if the clutch is slipping.

In all these cases, the speed of every gear and shaft inside the gearbox can be calculated from the wheel speed (or from the clutch output speeds  $\omega_{co1}$  and  $\omega_{co2}$ , for this last case) by considering the corresponding gear ratios.

When one of the clutches is closed, the case with only one degree of freedom must be considered: this condition is called “no-slip” condition. When both clutches are slipping or open, they both are in “slip” condition and the cases with more degrees of freedom must be taken into account. At every gear shift and drive away event the clutch passes from one condition to the other; the modeling issue is to provide continuity in the calculation of the clutch speed while changing its condition from “no slip” to “slip” and *vice versa*. When during the “slip” phase the engine speed and one of the clutch output speeds become equal, the relative clutch goes to “no-slip” condition, and the entire system gets only one degree of freedom. On the contrary, the switch from “no-slip” to “slip” condition happens when during the “no-slip” phase the engine torque becomes greater than the transmissible clutch torque calculated by the clutch torque model, because in these conditions the clutch is not able to transmit all the required torque anymore. This passage happens also when the clutch pressure is lower than the kiss point pressure, because the friction discs are not in direct contact with the clutch separator plates anymore.

## 1.9 Engine Model

The model presented in the previous paragraphs may be considered complete once all the vehicle parts generating and transmitting torque are simulated, from the engine to the wheels. The engine model implemented for real-time application is a real-time zero-dimensional mean value model (He and Lin, 2007), and comprehends the control logic of the Engine Control Unit (ECU). It can therefore maintain idle speed set-point during idling, and it can correctly respond to torque and speed requests coming from the TCU, when the ECU becomes “slave” and the DCT controller (TCU) becomes “master” (for example during drive away and gear shift operations). All CAN (Controller Area Network) bus messages between the ECU and TCU have been reproduced in simulation.

## 2 SIMPLIFIED MODEL FOR HIL APPLICATION

The presented model needs, as inputs, only the electrical currents from the TCU, the driver inputs (accelerator pedal, brake pedal pressure and gear shift request) and environmental data. However, it is not directly suitable for real-time application, because both the pressure dynamics and the mass-spring-damper dynamics are very fast, while there is a strict lower limit in the simulation step size: as the simulation must be real-time, the step size for the considered model should be set to around 0.5 ms. The simulation of the whole system with this step size may cause instability and undermine the possibility of plausible results.

To ensure stability of the simulation, the model must be tested under the worst conditions, which in this case are represented by a step current input on the clutch actuation valve, that forces the fastest pressure and motion dynamics, related one to each other. Hence, before comparing the simulation results to experimental data, the model was tested by performing a simulation of the clutch dynamics, having as input on the actuation valve a current step of 700 mA and considering progressively smaller step sizes: as shown in Figure 10, to avoid instability even a step size as small as 1  $\mu$ s may not be sufficient, and such value is absolutely not acceptable for a real-time application. Therefore, a simplification of the model dynamics is needed. The issue is to maintain the basic dynamic behavior, trying to recognize, isolate and modify only those parts that produce instability during real-time simulation.

Considering the mass-spring-damper dynamics of the valve spool, the instability is caused by the mass that is generally very small and determines a very large natural (and resonating) frequency of the system. The consequent oscillation is very fast and not reproducible in a

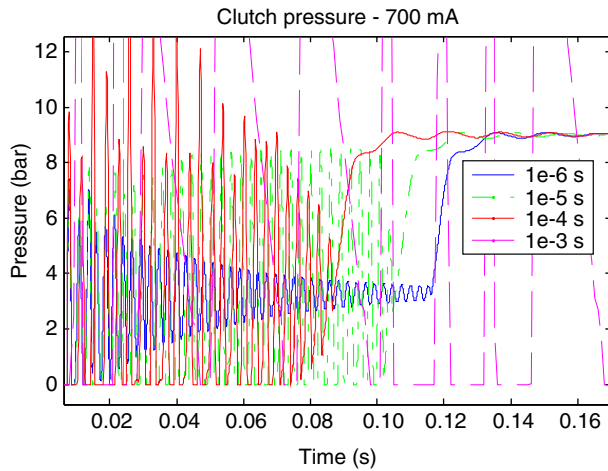


Figure 10

Analysis of simulation results while applying current steps with different simulation step sizes.

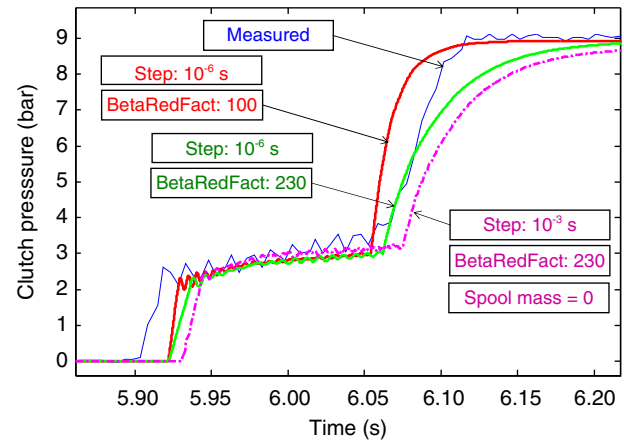


Figure 11

Simulation of clutch model with a fast current ramp from 0 to 700 mA.

real-time simulation. The solution that has been found is a “simplified dynamic equation” that does not consider masses anymore, and the viscous friction coefficient  $b_{sp}$  is replaced by a dummy  $b_{sp}^*$  much larger than the real one. Therefore, the second-order dynamic equation is simplified as a first-order dynamics ruled by the viscous coefficient and the spring stiffness. Equation (3) is replaced by Equation (44):

$$b_{sp}^* \dot{x}_{sp} + k_{sp} x_{sp} = F_{sol} - F_{fb} - F_{fl} - F_{pr-sp} \quad (44)$$

Instead, there is no need to simplify the dynamic equation of clutches and synchronizers, since their masses are large enough to prevent fast oscillations.

At the same time, the pressure dynamics in the different parts of the circuit are very fast, because the oil is theoretically incompressible and, even considering the theoretical value of the bulk modulus of the oil, a single drop of oil would be enough to raise the pressure to very large values in a single simulation step. Furthermore, in the real system other aspects must be taken into account: first of all, the effect of the percentage of air entrained inside the oil circuit (expressed in Eq. 45 as the ratio  $V_g/V_{tot}$ ) is not negligible, and leads to a significant decrease of the bulk modulus of the whole system  $\beta_{tot}$ , because the air bulk modulus  $\beta_g$  is very small:

$$\frac{1}{\beta_{tot}} = \frac{1}{\beta_{oil}} + \frac{V_g}{V_{tot}} \frac{1}{\beta_g} \quad (45)$$

The percentage of air inside the oil is not experimentally known, and the total bulk modulus should also

comprehend the stiffness of the pipes and the small leakages in the components (only the controlled leakage from the clutches to the oil sump is explicitly considered in the model). Therefore, the actual bulk modulus is much lower than the theoretical value, and the use of a lower value in the model, in order to allow a stable simulation of the system, can be considered physically realistic. The minimum equivalent value  $\beta_{tot}$  for a stable real-time simulation is 230 times lower than the theoretical value; it approximately corresponds to 1.4% of air volume inside the oil volume, which can be considered realistic.

In Figure 11, the effects of these two variations are separately analyzed, by comparing the model results with experimental data, measured while exciting the clutch control valve with fast current ramps, and analyzing the corresponding pressure ramps. First, the effect of the bulk modulus value is analyzed by comparing the results of simulations performed both with a step size of 1  $\mu$ s, that allows to freely modify the bulk modulus to match the results of an on board measure: with a bulk modulus reduction factor set to 100, the simulation with a step size of 1  $\mu$ s matches the measured pressure ramp; setting this value to 230 (the smallest reduction factor for a stable real-time simulation with step size of 0.5 ms) the pressure ramp is slower and reaches the steady-state value with a certain delay with respect to the measured signal, but such delay can be considered negligible for real-time application. The time delay between measured and simulated signals at the beginning of the pressure rise trend ( $t = 5.9$  s) is negligible for the proposed application, and it is mainly due to an overestimated circuit

volume fraction initially empty (to be filled with oil before the pressure can rise).

Despite all the simplifications introduced to reach a stable real-time simulation of a system with very fast dynamics, the model described in these paragraphs can be considered reliable for HIL applications. Before being implemented in the real-time application, a first offline calibration and validation of the model is needed.

### 3 OFFLINE SIMULATION RESULTS

The first analysis of the results obtained with the developed model, which comprehends all the different parts previously described, is made through an offline simulation, without the connection to the TCU; the input values (*i.e.* currents and driver's requests) are taken from measurements performed on board the vehicle. The simulation step size is set to 0.5 ms.

#### 3.1 Clutch Pressure

Clutch motion is a particularly delicate parameter to deal with (*Fig. 12*). When the clutch is open, the clutch pressure is maintained at a level greater than zero, to be ready for a quick closing actuation, but it is still completely open, thanks to the clutch spring preload. When the clutch is not moving, the clutch pressure is proportional to the input current on the clutch valve; it is the case of completely open clutch (until  $t = 27.35$  s) and completely closed clutch (from  $t = 27.60$  s). Answering a clutch closure request, the TCU provides a current peak for the clutch filling phase, the clutch valve's spool starts moving and the oil flows from the input port P to the actuation port A (*Fig. 3, 4*) and then to the clutch circuit: the pressure level in this circuit rises. The value reached before the complete clutch closure is proportional to the clutch spring stiffness. Once the clutch is completely closed, the TCU provides current to maintain the desired pressure level, calculated according to the torque that must be transmitted.

The validity of the simulation results can be verified by analyzing the clutch circuit pressure signal measured on board (this pressure level is called clutch pressure). As shown in *Figure 12*, the simulated pressure signal matches the measured one closely.

#### 3.2 System Pressure

The TCU controls the actuation current on the system pressure control valve according to the target pressure value. By supplying current to the valve, a controlled amount of oil is discharged to the low pressure circuit

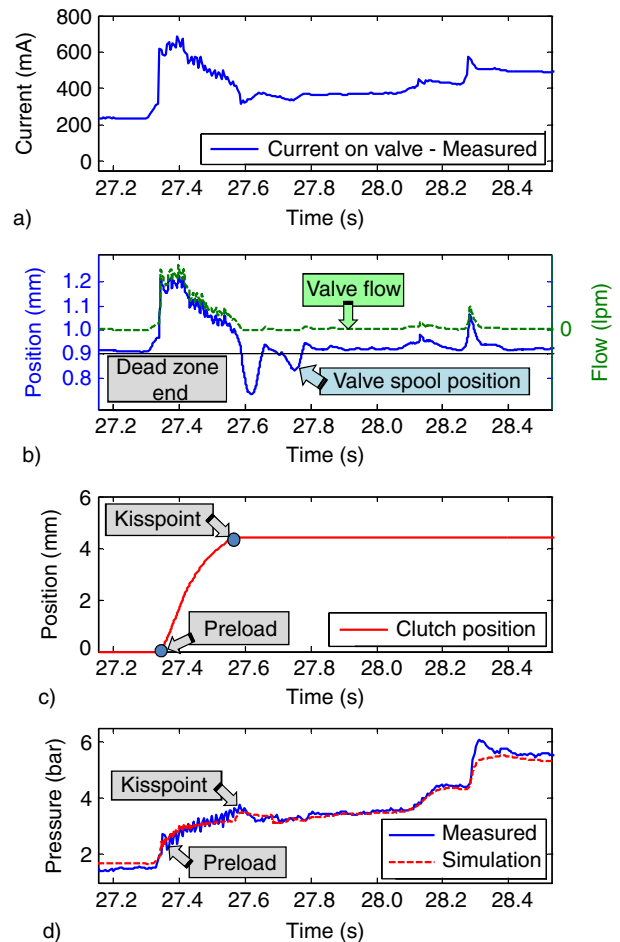


Figure 12

Offline simulation of clutch closing procedure.

from the high pressure circuit, causing a decrease of the system pressure level; all other flows (to the clutch pressure and to the rod pressure circuits) act as disturbances on the target system pressure, causing a quick fall of the pressure level; consequently, the actuation current is reduced by the TCU to maintain the desired pressure level. As in the clutch pressure simulation, the flows signals are not measured on board and the results of the simulation can be compared only with the pressure signal. The real-time simulation cannot reproduce the high frequency oscillations of the experimental measurements, but the obtained low-frequency content is correct (*Fig. 13*).

#### 3.3 Synchronizers

In *Figure 14*, the gear selection on the odd shaft of the transmission is shown; during all this process the engine

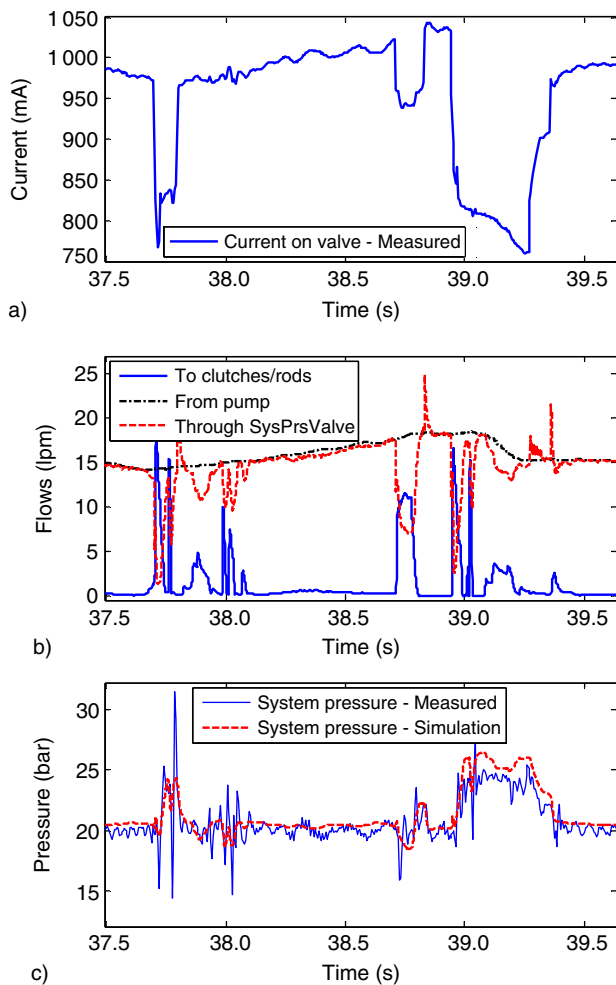


Figure 13  
Offline simulation of system pressure circuit.

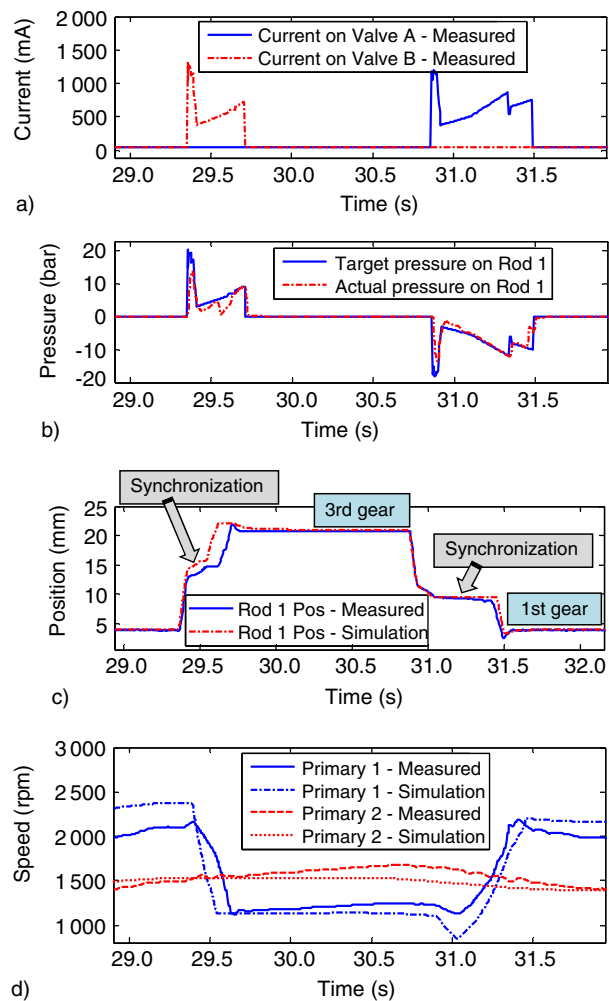


Figure 14  
Offline simulation of gear selection procedure.

is transmitting torque through the even shaft in 2<sup>nd</sup> gear, while the odd clutch is completely open; therefore, the engine speed and the even shaft speed are coincident. The pre-selection of gears is controlled by the TCU, which predicts the “future” gear according mainly to the engine speed trend and to the torque request. The simulation results can be evaluated by analyzing the rod position signals measured on board; in this case the pressure value inside the gear actuators is not measurable.

At first, rod 1 is engaging the 1<sup>st</sup> gear, which corresponds to the low position measured by the sensor (Fig. 14c, until  $t = 29.4$  s); when the TCU triggers the pre-selection of the 3<sup>rd</sup> gear, it provides on valve A (Fig. 2) an actuation current with a very impulsive shape (Fig. 14a, at  $t = 29.4$  s), in order to move the

synchronizer from the engaged position; then the current changes into a ramp profile when the 3<sup>rd</sup> gear (which corresponds to the high position measured by the sensor) is synchronizing (Fig. 14c, d, from  $t = 29.5$  s to  $t = 29.7$  s), to prevent the risk of gear scratching. The net pressure inside the rod (*i.e.* the difference between the pressure on the left chamber and the one on the right chamber, Fig. 14b), follows the target pressure imposed by the TCU; the oil flow from the rod pressure circuit to the rod chamber in the phases with a fast movement of the rod acts as a disturbance on this target pressure, because the movement determines a volume increase that must be filled by oil, causing a temporary pressure level decrease (Fig. 14b,  $t = 29.6$  s). When the speed synchronization is complete, the 3<sup>rd</sup> gear is correctly engaged and there is no more need for pressure in the rod chambers. At time

$t = 30.7$  s the engine starts slowing down and at time  $t = 30.9$  s the TCU triggers the pre-selection of 1<sup>st</sup> gear, pumping current to valve A and following the same procedure.

The simulation output matches the experimental one closely; the most difficult part is the simulation of the synchronization phase, because a closed loop control would be necessary to recognize the moment in which the gear is engaged and consequently reduce the input current.

#### 4 HARDWARE

The hardware chosen for the Hardware in The Loop application of the model developed during this project is based on a *dSPACE* “Mid-Size” Simulator, shown in Figure 15. It is equipped with a remote-controlled power supply unit (with an upper current limit of 50 A and a voltage regulation from 0 to 20 V controlled by the real-time system), a “ds1005” PPC board and two “ds2210” I/O boards, load cards, Failure Insertion Units (FIU) and ECU connectors.

The ds1005 PPC board comprehends a Real-Time Processor unit (RTP), RAM, flash and cache memory and timer interrupts, and is connected to the host PC. The PPC board is connected to the two I/O boards, containing sensors and actuators interfaces that provide a typical set of automotive I/O functions, including A/D conversion, digital I/O, and wheel speed sensor signal generation. In the application described in this paper, Analog/Digital Converter (ADC) is used for the actuation signals of proportional valves (pressure regulation of clutches, rods and electronic differential, and lubrication valves), Digital/Resistance converter (D/R) for temperature sensors, paddles and reverse button, Digital/Analog Converter (DAC) for pressure and position sensors, Pulse Width Modulation (PWM) signal generator for the actuation of on/off valves (clutch redundant valves, bypass, electric and hydraulic parking lock command); a CAN controller gives the possibility to set two



Figure 15  
*dSPACE* “Mid-Size” Simulator.

CAN lines per board. A load card permits the connection of the TCU to the loads it controls and actuates; the connected loads are the real valves and actuators of the DCT transmission, to obtain the best possible match with the real system. Each load channel is connected to a Failure Insertion Unit (FIU), to give the possibility to simulate failures in the TCU wiring. Three types of failure can be simulated: TCU output shorted to battery voltage, TCU output shorted to ground, and TCU output open circuit.

The developed Simulink model of the physical system has been integrated with a proper I/O conversion sub-model, as shown in Figure 16, in order to connect the physical model to the I/O boards. It is capable to convert the physical signals in electric signals, considering the characteristic of every sensor, and send them to the TCU. The actuation currents controlled by the TCU are read and sent as inputs to the model.

A graphical interface was developed using the *dSPACE* Control Desk environment in the host PC, to allow full control of the simulator also by inexperienced users. Figure 17 shows the dashboard interface, developed to provide into one single window all the main controls and indicators needed to perform manual tests.

#### 5 HIL APPLICATION RESULTS

The developed Simulink model is compiled with the use of “Real-Time Workshop” tool and then flashed inside the HIL real-time processor unit. The HIL application

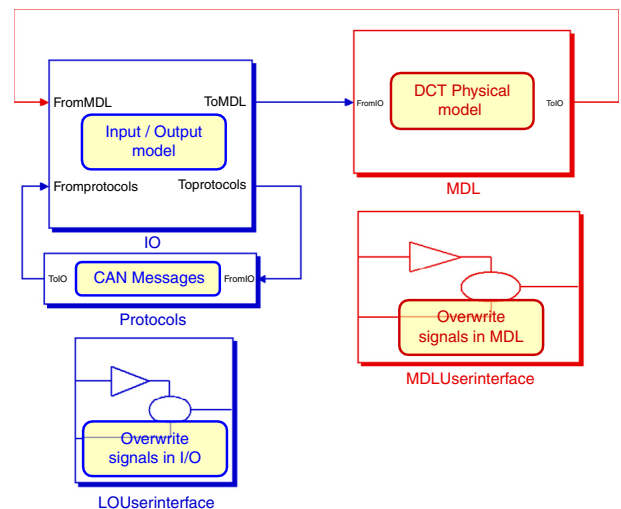


Figure 16  
Complete Simulink model.





Figure 17  
Dashboard interface.

permits to execute a wide range of tests to check and validate the functionality of the DCT controller; in general, these tests can be of different kinds. Functional tests permit to check the main functionality of the TCU, as drive away, gear shift, performance launch and interaction with the driver through paddles and buttons. The possibility of introducing a mechanical, hydraulic or electrical fault in the system allows verifying the TCU capability to recognize the problem and recover to a safe state. The capability of the controller to adapt to changes in the controlled system during its lifetime can be checked by analyzing the result of adaptation procedures.

## 5.1 Functional Tests

First of all, the basic functions implemented in the TCU have been tested. In a dual clutch transmission, the gear shift is performed only opening the offgoing clutch and closing the ongoing one, thanks to the possibility of pre-selecting gears on odd and even shaft before the gear shift. Figure 18 considers a gear shift from 3<sup>rd</sup> to 4<sup>th</sup> gear.

Figure 18a shows the pressure profile during the gear shift. The clutch torque transmitted by the offgoing clutch (clutch n.1 or “odd” clutch) is reduced at the beginning of the gear shift (time 160.7 s), by reducing the pressure in the clutch actuation; at the same time, the TCU starts pumping current on the ongoing clutch (clutch n.2 or “even” clutch); in this transient (time between 160.7 s and 161.1 s), the clutch pressure is not proportional to the current supplied to the proportional valve, because the oil is filling the clutch, which is moving forward towards the kiss point position, maintaining a low pressure value with high current on the valve. At time 161.1 s, the clutch kiss point is reached in the even clutch; the current on the even proportional valve is reduced and the pressure on the two clutches is regulated to achieve the best shift comfort; the two pressure signals are crossing themselves, in a way that some torque is

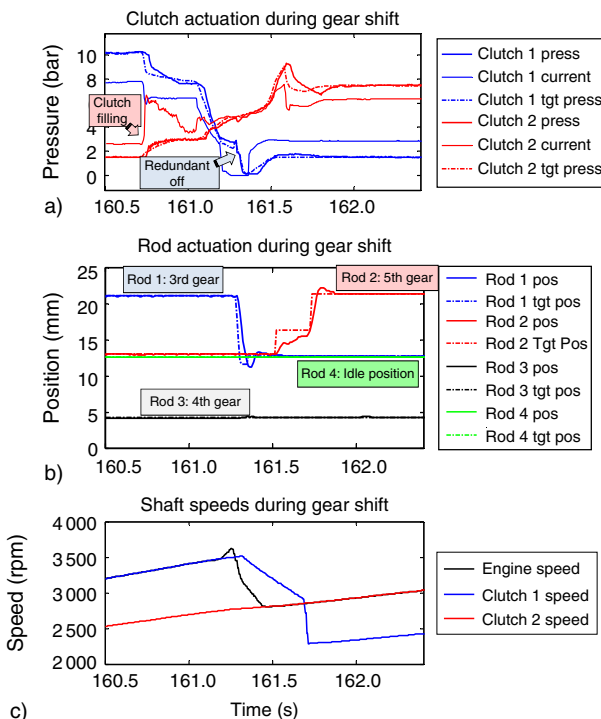


Figure 18  
Gear shift from 3<sup>rd</sup> to 4<sup>th</sup> gear.

always transmitted during all the gear shift and the wheels are never left without torque: the torque interruption during gear shift typical of MT and AMT is eliminated. At the end of the process, the pressure in the odd clutch is discharged as fast as possible by connecting the relative redundant valve to the sump, to ensure a complete clutch opening; the valve is then actuated again, and the pressure level in the clutch actuation is maintained at around 1.5 bar, ready for the next gear shift.

The actual pressures calculated by the simulator are able to follow the target ones closely. A small delay can be noticed between the simulated signals and the target ones (set by the TCU) during the fastest transients; this delay is due to the simplifications needed for a real-time simulation, and it is small enough not to affect the TCU control.

In Figure 18b, the rod actuation is shown. During all the gear shift process, the rods of the even gears are not moved; the 4<sup>th</sup> gear (correspondent to a low position of rod 3) was already selected before the gear shift, while the even shaft was not transmitting torque because its clutch was open; the odd gear is closed and transmitting torque in 3<sup>rd</sup> gear (rod 1 in high position). As soon as the oil inside the odd clutch is discharged by the redundant

valve, the 3<sup>rd</sup> gear is deselected, moving the correspondent rod from engaged to idle position, pumping current on the correspondent valve. Then, while the odd clutch is open, the rod 2 is moved to preselect the 5<sup>th</sup> gear (high position), ready for the next gear shift. During the gear shift the TCU is “master” and the engine ECU is “slave”; this means that the target engine speed and torque are set by the TCU. The engine speed follows the odd clutch speed as far as the odd clutch pressure is not reduced; then, after accelerating for a short while to improve the driver’s feeling, it reaches the even clutch speed during the closure of the even clutch (Fig. 18c). Meanwhile, the odd clutch speed slows down, reaching the speed correspondent to the 5<sup>th</sup> gear as soon as the synchronization process is complete.

## 5.2 Mechanical Failures Simulation

Figure 19 shows the simulation of a problem with the synchronizer of 1<sup>st</sup> and 3<sup>rd</sup> gear: in the real system, there is the possibility that the synchronizer cones would not transmit the usual torque to the gear anymore; it can happen because of unusual wear (the durability of the cone friction material is not infinite), or when, due to some failure in the clutch actuation circuit, during the selection of the gear some torque is transmitted by the engine to the primary shaft, and consequently to

the gear; in this condition the cones covered with friction material heat up abnormally and lose their friction characteristic. In both cases, the effect is the loss of capacity in synchronizing the speed of synchronizer (and output shaft) and gear (rigidly connected to the input shaft). This behavior is simulated inside the model setting to zero the friction coefficient on the specific cones. Consequently, the synchronizer cannot select the gear anymore; the TCU detects a problem with the gear, tries the engagement other three times consecutively, pumping all the possible pressure inside the piston of the rod; if the procedure is not successful, the TCU validates the failure identification and sets the recovery mode, that consists in the impossibility to select that particular gear.

In Figure 19b, the 3<sup>rd</sup> gear cannot be selected, and after three more attempts the gearbox shifts directly from 2<sup>nd</sup> to 4<sup>th</sup> gear. This gear shift, in which offgoing and ongoing gears are both on the same shaft, is performed with torque interruption: the even clutch is opened, 2<sup>nd</sup> gear (rod 4 in high position) is deselected and 4<sup>th</sup> gear is selected (rod 3 in low position), then the even clutch is closed again (Fig. 19a, from time 27.5 s). During the three trials, the odd shaft is not correctly moving to the speed of 3<sup>rd</sup> gear (Fig. 19c); immediately after the TCU has set the error, the 5<sup>th</sup> gear is preselected on it.

## 5.3 Hydraulic Failure Simulation

Figure 20 shows a failure due to an anomalous pressure drop in the odd clutch actuation: it can be caused by an augmented leakage flow from the actuation chamber to the sump, due to a broken hydraulic seal in the clutch actuation piston, or because the pressure regulation valves, the proportional one or the redundant one, are stuck and their spools cannot move properly anymore when actuated with a certain current. All these kinds of failures can be simulated in the model.

Before the failure injection, a gear shift from 2<sup>nd</sup> to 3<sup>rd</sup> gear is performed, and the odd clutch is being closed, reaching the engine speed. When the failure is inserted in the system, the pressure level drops and the clutch cannot transmit to the wheels all the torque provided by the engine anymore; consequently, the engine speed cannot follow the odd clutch speed and the engine shaft starts revving up. The TCU recognizes that the actual odd clutch pressure is not following the target pressure; the consequent action is the closure of both redundant and proportional valves which control the odd clutch; the odd gear selection is then excluded and the respective synchronizers are put in idle position, to disconnect the odd primary shaft from the wheels.

From this moment, only the even clutch can be used; not to leave the car without torque on the wheels,

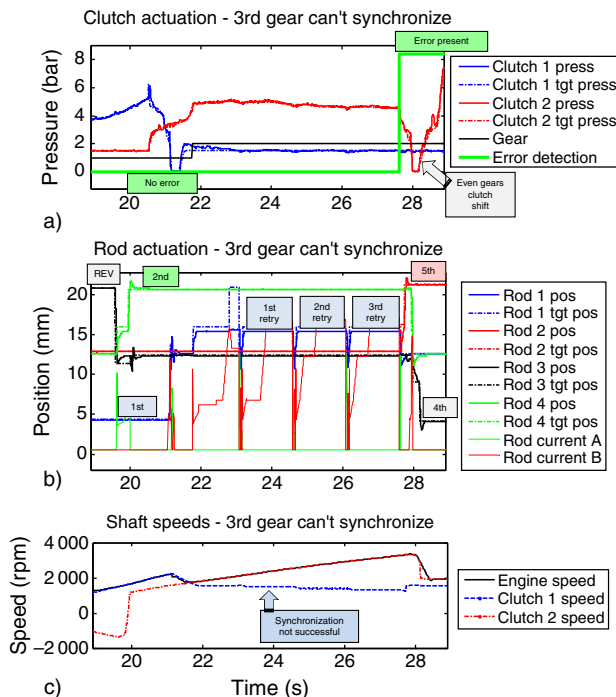


Figure 19

Failure while synchronizing 3<sup>rd</sup> gear.

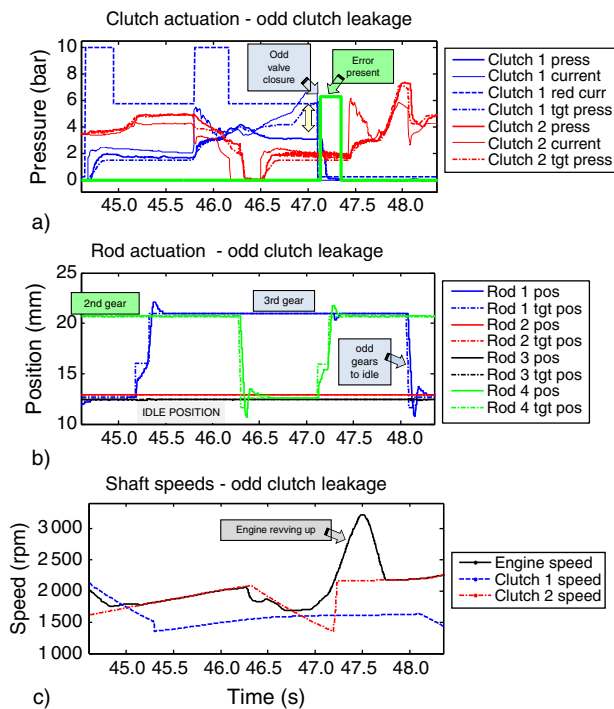


Figure 20

Failure in the odd clutch hydraulic actuation.

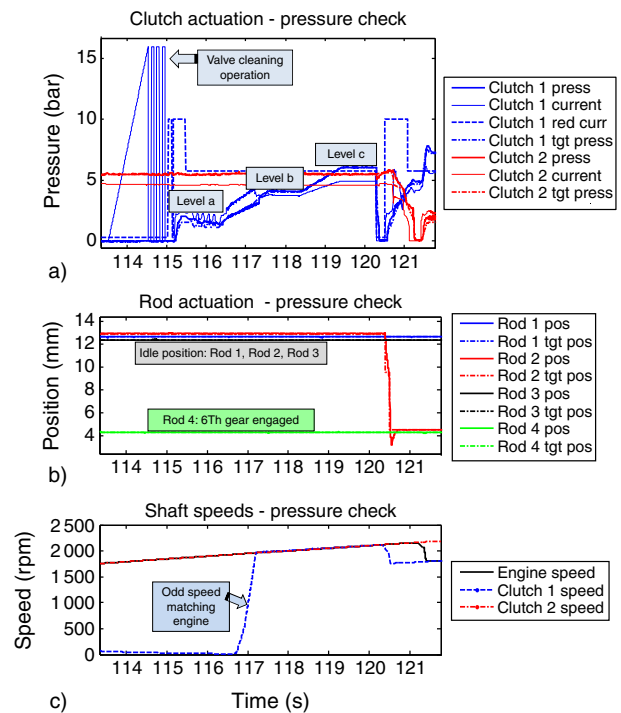


Figure 21

Recovery after failure in the hydraulic actuation of odd clutch.

the even clutch is closed immediately after recognizing the failure, performing an automatic gear shift not requested by the driver. The engine speed slows down, matching the even shaft speed.

The TCU regularly tries to restore the full functionality of the gearbox (Fig. 21), checking if the clutch actuation is capable again to give the desired pressure; a procedure of valve cleaning is performed on both the proportional and redundant odd valves, shaking them with an impulsive actuation (Fig. 21a, from time 114.5 s to time 115.1 s); then, the TCU checks if the proportional valve can provide the desired pressure level again, setting three different levels of target pressure to follow (A, B, C). During this test both the synchronizers of odd gears are maintained in idle position (Fig. 21b); the odd clutch speed joins the engine speed because the clutch is being closed (Fig. 21c). If the actual pressure follows the target pressure correctly, the complete functionality of the gearbox is restored.

#### 5.4 Electrical Failure Simulation

The reproduction of electrical failures is a core aim of HIL applications; tests that would be complicated,

time consuming and cost relevant on the real system can be rapidly carried out on the simulated system. Thanks to the Failure Injection Unit (FIU) described in the previous paragraphs, it is possible to simulate electrical faults – short to battery, short to ground, open circuit – on all the actuation valves and on all the sensor signals.

Figure 22 shows a failure imposed on the system pressure actuation valve (*i.e.* the valve that regulates the pressure level in the high pressure circuit): at time 9.9 s the actuation wiring is shorted to ground. Before the failure injection, the system pressure is regulated at 15 bar by the TCU; when the electrical failure occurs, the valve cannot be kept open anymore, because no current can be supplied to it, being connected to the ground. Consequently, the oil cannot flow from the high pressure circuit to the low pressure one anymore, but at the same time the input flow from the pump cannot be stopped because the pump is rigidly connected to the engine. The amount of oil flowing inside the circuit cannot be discharged, and the pressure level rises, reaching a value of around 40 bar, level at which the safety hydraulic valve present inside the circuit opens, permitting to discharge some oil to the sump. In the meanwhile,

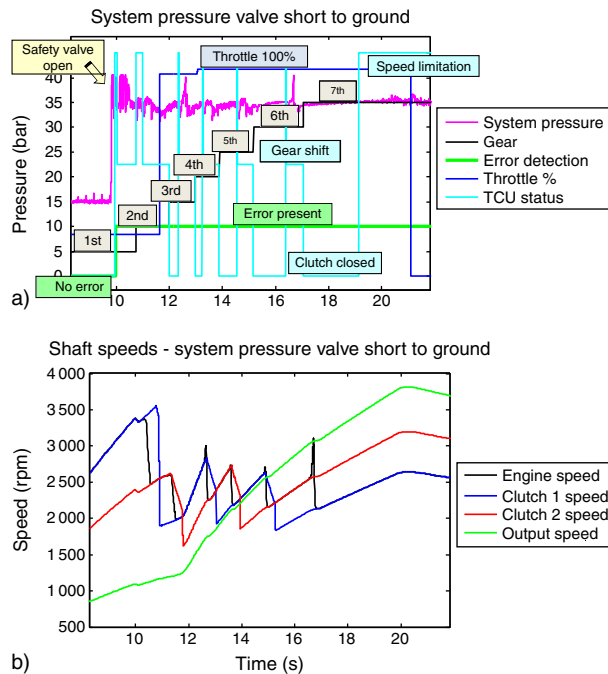


Figure 22

Simulation of electrical failure on system pressure regulation valve.

the TCU recognizes the failure in the electrical circuit and sets its recovery operation: in order to reduce the engine speed, and consequently the flow from the pump, consecutive gear shifts are performed. When the 7<sup>th</sup> gear is reached, the engine speed is limited by the TCU in order to maintain an acceptable pressure level inside the circuit.

## 6 ADAPTION PROCEDURES

To perform a precise and comfortable control of the transmission, every TCU must be adapted to the gearbox it is connected to; this is the reason why some “end of line” calibrations of the TCU are needed after coupling a TCU to a specific gearbox. The adaption procedures comprehend rod calibration, clutch preload and kiss point detection, clutch filling procedure, and detection of the solenoid characteristic of proportional clutch pressure regulation valves. These procedures are regularly performed by the TCU during its lifetime: the adaptive values can change from the ones identified with a new gearbox, because of many factors, such as wear, flexion of mechanical parts, augmented leakage in the hydraulic circuit, and change in oil properties. In the

HIL application, the characteristic of the components inside the model can be changed as desired; it is then possible to check the capability of the TCU to correctly adapt to the new settings, updating its calibrations to new values.

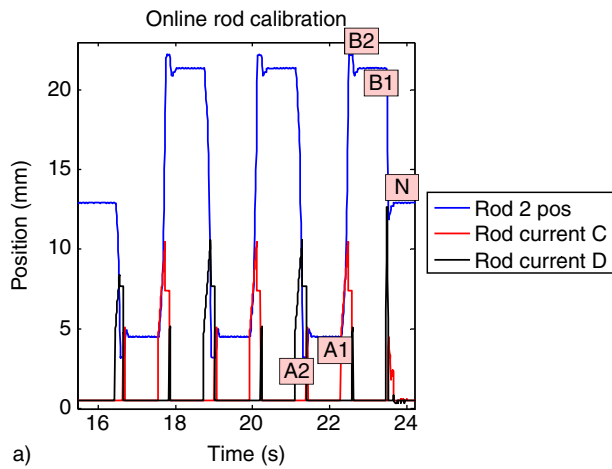
### 6.1 Rod Calibration

Figure 23a shows the adaption procedure on rod number 2. The calibration of a rod consists in moving the synchronizer from its idle position, forcing it to engage both of the gears it controls, and checking the 5 characteristic steady-state positions of the rod: idle position (N), gear engaged with pressure acting on the synchronizer (A2, B2), engaged gear without pressure on the synchronizer (A1, B1), on each of the two gears. It is performed three times per gear and the mean values of the 3 trials are memorized in the TCU as the adapted positions. During the gearbox lifetime, the TCU recognizes a failure in the synchronizer actuation when the position measured from the sensor does not match the expected one registered during the online self-calibration. The simulation results show a good capability of the TCU to adapt to the values set in the model; Figure 23b shows the original values memorized inside the TCU (on the left), and the new values registered by the TCU during the adaption procedure (on the right).

### 6.2 Detection of Clutch Valve Solenoid Characteristic

To perform an accurate pressure control in the clutch actuation circuit, the TCU needs to know with a high level of accuracy the current–pressure characteristic of the proportional valves that regulate the clutch actuation. For this reason, a default map is not sufficient, and the characteristic must be adapted to the specific hydraulic valve and plate. The solenoid characteristic adaption procedure shown in Figure 24a is performed by the TCU by setting different steady-state target pressure values to be reached inside the clutch actuation chamber, and measuring the input current needed to reach them. This procedure is performed for both clutches, and with all the rods in idle position. A correction map is then calculated to adapt the default map; the input value to the correction map is the default current calculated by the TCU, the output value is the correction to impose on the current itself to perform a precise actuation. The simulation results confirm the capability of the TCU to react to the characteristic being simulated in the model. Figure 24b shows the difference between the previous correction map and the last one, memorized after the adaption procedure.





Rod1_PosA2_Default	3231	Rod1_PosA2_Adp	3057 (um)
Rod1_PosA1_Default	4526	Rod1_PosA1_Adp	4320 (um)
Rod1_PosN_Default	12708	Rod1_PosN_Adp	12649 (um)
Rod1_PosB1_Default	21081	Rod1_PosB1_Adp	20994 (um)
Rod1_PosB2_Default	22094	Rod1_PosB2_Adp	22042 (um)
Rod2_PosA2_Default	3251	Rod2_PosA2_Adp	3241 (um)
Rod2_PosA1_Default	4468	Rod2_PosA1_Adp	4520 (um)
Rod2_PosN_Default	12533	Rod2_PosN_Adp	12925 (um)
Rod2_PosB1_Default	20992	Rod2_PosB1_Adp	21339 (um)
Rod2_PosB2_Default	21758	Rod2_PosB2_Adp	22169 (um)
Rod3_PosA2_Default	3373	Rod3_PosA2_Adp	3036 (um)
Rod3_PosA1_Default	4773	Rod3_PosA1_Adp	4293 (um)
Rod3_PosN_Default	13066	Rod3_PosN_Adp	12395 (um)
Rod3_PosB1_Default	21437	Rod3_PosB1_Adp	20934 (um)
Rod3_PosB2_Default	22268	Rod3_PosB2_Adp	21973 (um)
Rod4_PosA2_Default	3198	Rod4_PosA2_Adp	3028 (um)
Rod4_PosA1_Default	4545	Rod4_PosA1_Adp	4295 (um)
Rod4_PosN_Default	12716	Rod4_PosN_Adp	12598 (um)
Rod4_PosB1_Default	20965	Rod4_PosB1_Adp	20707 (um)
Rod4_PosB2_Default	21906	Rod4_PosB2_Adp	21754 (um)

Figure 23

a) Calibration procedure of rod 2; b) comparison between default and adapted values.

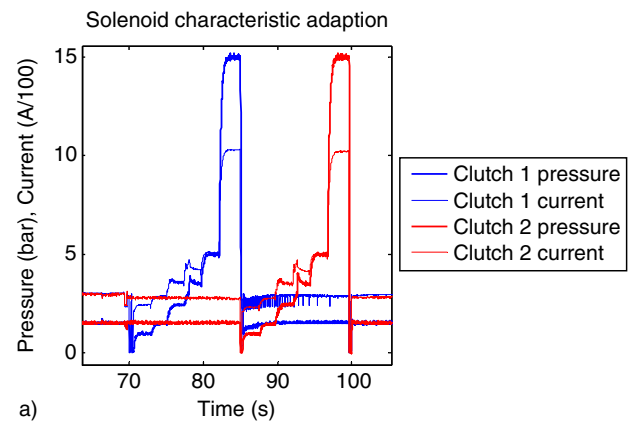


Figure 24

a) Adaption of clutch actuation circuit; b) comparison between default values (white background) and adapted values (gray background).

## 7 AUTOMATION OF TESTS

All the tests on the Hardware In the Loop application have been initially performed manually with the use of the real-time interface. A list of tests has then been defined and every test in the list has been automated. A script developed in Python software environment controls the communication with the simulator, giving the proper commands and inserting the needed failures. During the test, all the relevant signals are automatically recorded in a .dat file, while a .txt log registers the error codes and the environmental conditions thanks to a diagnostic interface. During the post-processing stage, a Matlab code checks automatically the .dat measures one by one, according to a .xls file where all the condi-

tions to be checked had previously been defined. Only if all the conditions are fulfilled, the test is passed. This automation chain allows performing a large number of tests without human interaction. When the pattern of automatic tests is large enough, a complete validation of new software releases can be performed automatically.

## CONCLUSIONS

A control oriented model of a Dual Clutch Transmission (DCT) has been developed, by considering the dynamic physical equations of hydraulic circuit, clutches and synchronizers, of all the shafts inside the gearbox



(considered with infinite stiffness), and a vehicle model that takes into account the resistant forces acting on the vehicle and inertia effects. The different parts of the model were at first tested and validated separately; a simplification of some dynamics was carried out to adapt the model to real-time applications, in order to reproduce the fast dynamics of the hydraulic circuit while maintaining a sufficiently large simulation step size.

To validate the DCT model, the results of offline simulation of clutch pressure, system pressure, rod motion and shafts speeds have been compared to on-board measurements. An input/output signal scaling sub-model was then added, and the complete model was finally implemented in a HIL simulator, composed of a real-time processor, input/output boards, a TCU plate and a load plate.

Several tests have been performed on the HIL simulator: functional tests, as well as mechanical, hydraulic and electrical failure tests have been executed, analyzing the behavior of the model and the transmission control unit reaction. Adaption procedures were performed to verify the TCU ability to correctly adapt to specific gearbox characteristics (simulated by the HIL application). The results demonstrate the capability of the HIL model to correctly simulate the behavior of the real system, and to respond to the requests coming from the TCU both during functional tests and during failure recovery procedures.

A test automation procedure has been developed to meet the requirement of performing a pattern of tests without the direct interaction of the user. Tests automation allows saving time, reproducing identical tests on different software releases, and designing tests with a tight actions timing – sometimes with just a few milliseconds between them – that would not be possible to be executed manually by the user. Once a pattern of automatic tests can be considered complete, (*i.e.* once it stimulates all the relevant TCU functionalities), a fully automatic non-regression validation of the TCU software is possible in a safe, time-saving and cost-effective simulation environment.

## REFERENCES

- Bertotti G., Mayergoz I.D. (2006) *The Science of Hysteresis: Mathematical modeling and applications*, Academic Press, Germany, ISBN: 978-0-080-54078-8.
- Cavina N., Olivi D., Corti E., Poggio L., Marcigliano F. (2012) Development of a Dual Clutch Transmission Model for Real-Time Applications, *2012 IFAC Workshop on Engine and Powertrain Control, Simulation and Modeling Vol. 3*, Part 1, France, pp. 440-447, ISBN: 978-3-902823-16-8. DOI: 10.3182/20121023-3-FR-4025.00006.
- Cavina N., Olivi D., Corti E., Mancini G., Poggio L., Marcigliano F. (2013) Development and implementation of Hardware In the Loop simulation for Dual Clutch Transmission Control Units, *SAE Int. J. Passeng. Cars – Electron. Electr. Syst.* **6** 2, 458–466, DOI: 10.4271/2013-01-0816.
- Davis C.L., Sadeghi F., Krousgrill C.M. (2000) A Simplified Approach to Modeling Thermal Effects in Wet Clutch Engagement: Analytical and Experimental Comparison, Congrès STLE/ASME Tribology Conference, Orlando, FL, 10 Nov. 1999, *J. Tribol.* **122**, 1, 110-118, DOI:10.1115/1.555370.
- Deur J., Petric J., Asgari J., Hrovat D. (2005) Modeling of Wet Clutch Engagement Including a Thorough Experimental Validation, *SAE Technical Paper* 2005-01-0877, DOI: 10.4271/2005-01-0877.
- Eyabi P., Washington G. (2006) Nonlinear Modeling of an Electromagnetic Valve Actuator, *SAE Technical Paper* 2006-01-0043, DOI: 10.4271/2006-01-0043
- Goetz M., Levesley M.C., Crolla D.A. (2005) Dynamics and control of gearshifts on twin-clutch transmissions, *Proc. of the IMECHE, Part D: J. Automobile Engineering* **219**, 951-962.
- Greenwood J.A., Williamson J.B.P. (1966) Contact of nominally flat surfaces, *Proceedings of the Royal Society of London Series A, Mathematical and Physical Sciences* **295**, 1442, 300-319, DOI: 10.1098/rspa.1966.0242.
- Guzzella L., Onder C.H. (2004) *Introduction to Modeling and Control of Internal Combustion Engine Systems*, Springer, ISBN: 978-3-642-10775-7.
- Guzzella L., Sciarretta A. (2008) *Vehicle Propulsion Systems*, Springer, ISBN: 978-3-642-35913-2.
- He Y., Lin C. (2007) Development and Validation of a Mean Value Engine Model for Integrated Engine and Control System Simulation, *SAE Technical Paper* 2007-01-1304, DOI: 10.4271/2007-01-1304.
- Kulkarni M., Shim T., Zhang Y. (2007) Shift dynamics and control of dual-clutch transmissions, *Mechanism and Machine Theory* **42**, 2, 168-182, DOI: 10.1016/j.mechmachtheory.2006.03.002.
- Lai G.Y. (2007) Simulation of heat-transfer characteristics of wet clutch engagement processes, *Numerical Heat Transfer, Part A: Applications* **33**, 6, 583-597, DOI: 10.1080/10407789808913956.
- Liu Y., Qin D., Jiang H., Zhang Y. (2009) A Systematic Model for Dynamics and Control of Dual Clutch Transmissions, *Journal of Mechanical Design* **131**, 6, 061012, DOI: 10.1115/1.3125883.
- Lucente G., Montanari M., Rossi C. (2007) Modelling of an automated manual transmission system, *Mechatronics* **17**, 2-3, 73-91, DOI: 10.1016/j.mechatronics.2006.11.002.
- Matthes B. (2005) Dual Clutch Transmissions – Lessons learned and future potential, *SAE Technical Paper* 2005-01-1021, DOI:10.4271/2005-01-1021.
- Merritt H.E. (1967) *Hydraulic Control Systems*, John Wiley and Sons Inc, ISBN: 978-0-471-59617-2.
- Montanari M., Ronchi F., Rossi C., Tilli A., Tonielli A. (2004) Control and performance evaluation of a clutch servo system with hydraulic actuation, *Control Engineering Practice* **12**, 11, 1369-1379, DOI: 10.1016/j.conengprac.2003.09.004.
- Naunheimer H., Bertsche B., Ryborz J., Novak W. (2011) *Automotive Transmissions: Fundamentals, Selection, Design and Application*, Springer, ISBN 978-3-642-16214-5

Neto D.V., Florencio D.G., Fernandez J., Rodriguez P. (2006) Manual Transmission: Synchronization Main Aspects, *SAE Technical Paper* 2006-01-2519, DOI:10.4271/2006-01-2519.

Razzacki S.T. (2004) Synchronizer Design: A Mathematical and Dimensional Treatise, *SAE Technical Paper* 2004-01-1230, DOI: 10.4271/2004-01-1230.

Velardocchia M., Amisano F., Flora R. (2000) A Linear Thermal Model for an Automotive Clutch, *SAE Technical Paper* 2000-01-0834, DOI:10.4271/2000-01-0834.

Zhang Y., Chen X., Zhang X., Jiang H., Tobler W. (2005) Dynamic Modeling and Simulation of a Dual Clutch Automated Lay-Shaft Transmission, *ASME Journal of Mechanical Design* **127**, 2, 302-307, DOI: 10.1115/1.1829069.

*Manuscript accepted in December 2013*

*Published online in April 2014*

**Cite this article as:** N. Cavina, E. Corti, F. Marcigliano, D. Olivi and L. Poggio (2015). Control-Oriented Models for Real-Time Simulation of Automotive Transmission Systems, *Oil Gas Sci. Technol* **70**, 1, 67-90.

© 2014. Notwithstanding the ProQuest Terms and conditions, you may use this content in accordance with the associated terms available at

<http://ogst.ifpenergiesnouvelles.fr/articles>